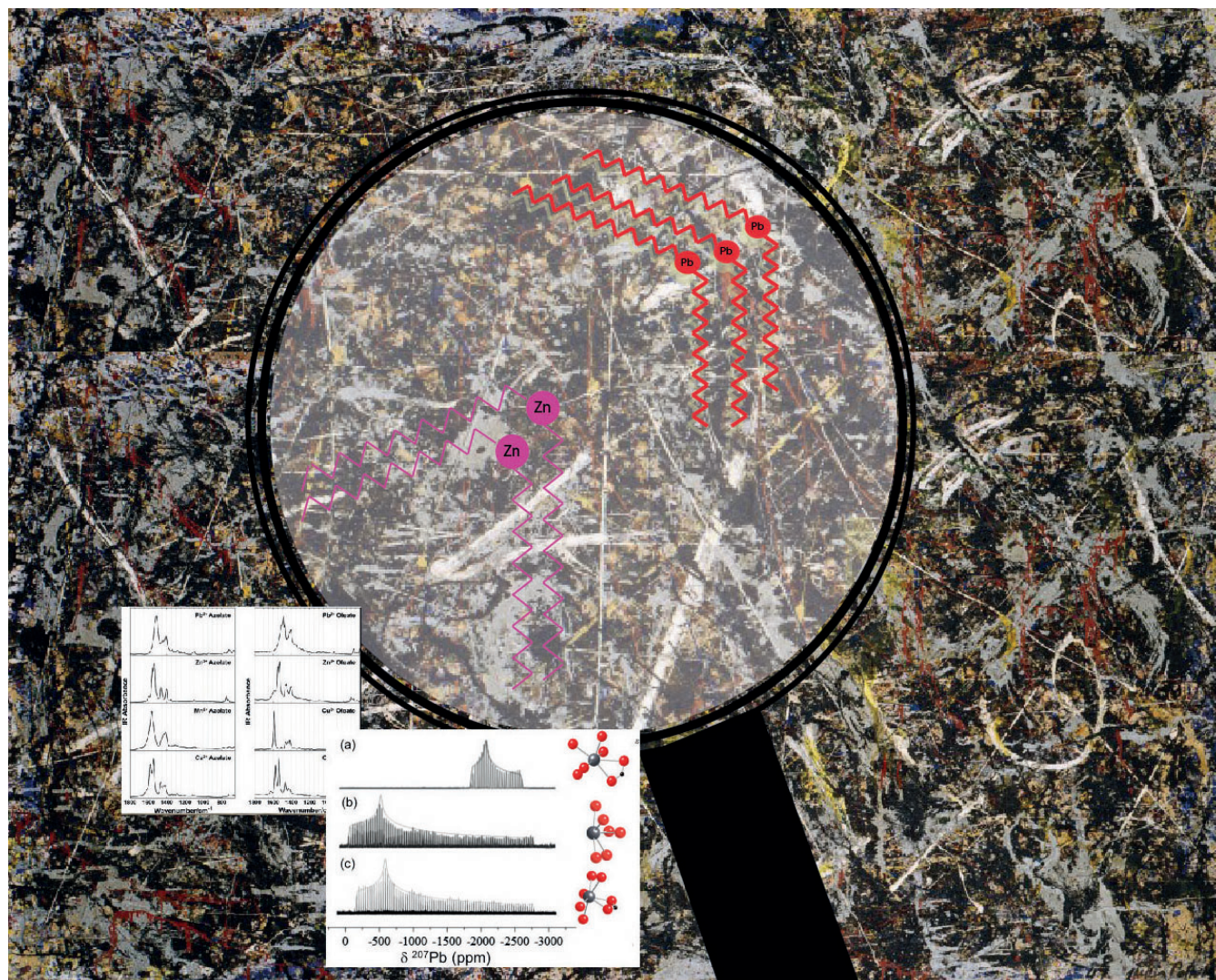


# A Critical Review on the Analysis of Metal Soaps in Oil Paintings

Francesca Caterina Izzo,<sup>\*,[a]</sup> Matilde Kratter,<sup>[b]</sup> Austin Nevin,<sup>[c]</sup> and Elisabetta Zendri<sup>[d]</sup>



Up to 70% of the oil paintings conserved in collections present metal soaps, which result from the chemical reaction between metal ions present in the painted layers and free fatty acids from the lipidic binders. In recent decades, conservators and conservation scientists have been systematically identifying various and frequent conservation problems that can be linked to the formation of metal soaps. It is also increasingly recognized that metal soap formation may not compromise the integrity of paint so there is a need for careful assessment of

the implications of metal soaps for conservation. This review aims to critically assess scientific literature related to commonly adopted analytical techniques for the analysis of metal soaps in oil paintings. A comparison of different analytical methods is provided, highlighting advantages associated with each, as well as limitations identified through the analysis of reference materials and applications to the analysis of samples from historical paintings.

## 1. Introduction

At the end of 1990s, an analytical campaign carried out during the restoration of the masterpiece *The Anatomy Lesson of Dr Nicolaes Tulp* by Rembrandt van Rijn, in the collection of the Royal Cabinet of Paintings, the Mauritshuis, in The Hague (The Netherlands) led to the report of numerous crater-like holes on the surface of the painting, the diameter of which ranged between 100 and 200  $\mu\text{m}$ . The term “protrusion” was coined to identify this phenomenon.<sup>[1]</sup> Although similar protrusions were observed in the 1970s, it was thanks to the MOLART (Molecular Aspects of Aging in Painted Works of Art) (1995–2002) and De Mayerne (2002–2006) research programs, sponsored by the Netherlands Organization for Scientific Research (NWO), that these protrusions were first analysed using advanced scientific methods. MOLART’s attention for this phenomenon was strongly inspired through work by Noble who recognised similar phenomena in other paintings.<sup>[2]</sup> The researchers involved in MOLART adopted a molecular approach to the study of the ageing processes in paintings leading to new insights that determined that the holes were caused by the aggregation of lead carboxylates which had previously formed due to the saponification of the lead-containing compounds in the paint system.<sup>[3,4]</sup> It was observed in paintings that the saponification of the lead-containing compounds not only

caused protrusions, but also increased the transparency of the paint and its brittleness, created efflorescence and led to paint losses, delamination and even cracks.<sup>[3,5]</sup> All these degradation signs were recognised as a consequence of the formation of metal soaps.<sup>[4]</sup>

In 2002, Noble and Boon designed a questionnaire that was sent to conservators and restorers: they intended to know if phenomena like those observed in *The Anatomy Lesson of Dr Nicolaes Tulp* were present in other paintings around the world. In this way, they could understand the extent of the presence of metal soaps. The results from the questionnaires were, then, published.<sup>[6]</sup> The first identification of metal soaps was just “the tip of the iceberg”;<sup>[7]</sup> conservators and restorers understood that the problem was worldwide spread. Since then, more and more cases of metal soaps have been recorded with a wide geographical distribution (from Europe to the United States, to Australia) and not only on canvas but also on artworks on copper, wood, paper, ivory and glass.<sup>[1,8]</sup> Further scientific investigations found that masterpieces by Pablo Picasso, Vincent van Gogh, Lucio Fontana, Willem de Kooning, Karel Appel, Jackson Pollock, Georgia O’Keeffe and Max Beckmann, just to cite some examples, were affected by the presence of metal soaps.<sup>[9–15]</sup> Metal soaps may cause several undesirable and often irreversible changes in the painting’s appearance: the abovementioned protrusions on the surface, the presence of efflorescence, darkening or contrarily translucency, losses, delamination and cracking.<sup>[16–21]</sup> While metal soaps are often related to degradation phenomena in oil paintings, thus influencing the stability of the painted systems. Nevertheless, it was observed that, sometimes, their presence does not produce any significant effect in multilayered paint films.<sup>[13,16]</sup> In this sense, the review by Cotte and co-authors on lead soaps clearly highlights how conservators and scientists have perceived metal soaps as either “foes” or “friends”, according to their “negative” impact (protrusions, efflorescences, darkening, etc) or their “positive” influence in the drying process.<sup>[22]</sup>

The impact of metal soaps on the conservation of paintings and the development of the scientific methods for their study was the focus of the symposium entitled *Metal soaps in Art*, held at the Rijksmuseum in Amsterdam in 2016.<sup>[23]</sup>

As reflected in the questionnaires by Noble and Boon, scientific investigations have demonstrated that metal soaps form preferentially in oil paintings, while few studies reported soaps in egg yolk or beeswax.<sup>[24–27]</sup> Moreover, lead and zinc soaps are the most commonly reported metal soaps, almost always bound to saturated fatty acid chains such as hexadeca-

- [a] Prof. F. C. Izzo  
Sciences and Technologies for the Conservation of Cultural Heritage,  
Department of Environmental Sciences, Informatics and Statistics  
Ca’ Foscari University of Venice  
Via Torino 155/b, 30173 Venice (Italy)  
E-mail: fra.izzo@unive.it
- [b] M. Kratter  
Sciences and Technologies for the Conservation of Cultural Heritage,  
Department of Environmental Sciences, Informatics and Statistics  
Ca’ Foscari University of Venice  
Via Torino 155/b, 30173 Venice (Italy)
- [c] Dr. A. Nevin  
Head of Conservation The Courtauld Institute of Art  
Vernon Square, Penton Rise  
Kings Cross, WC1X 9EW London (United Kingdom)
- [d] Prof. E. Zendri  
Sciences and Technologies for the Conservation of Cultural Heritage,  
Department of Environmental Sciences, Informatics and Statistics  
Ca’ Foscari University of Venice  
Via Torino 155/b, 30173 Venice (Italy)

© 2021 The Authors. Published by Wiley-VCH GmbH. This is an open access article under the terms of the Creative Commons Attribution Non-Commercial License, which permits use, distribution and reproduction in any medium, provided the original work is properly cited and is not used for commercial purposes.

noic ( $\text{CH}_3(\text{CH}_2)_{14}\text{COOH}$ ) (palmitic), octadecanoic ( $\text{C}_{17}\text{H}_{35}\text{CO}_2\text{H}$ ) (stearic) and nonanedioic ( $\text{C}_9\text{H}_{16}\text{O}_4$ ) (azelaic) acids.<sup>[22,28]</sup> Lead and zinc have also been reported bound to unsaturated fatty acid chains, such as (9Z)-octadec-9-enoic ( $\text{C}_{18}\text{H}_{34}\text{O}_2$ ) (oleic) acid.<sup>[29]</sup> In addition to lead and zinc soaps, other metal soaps, such as copper and potassium soaps, were less commonly detected.<sup>[1,4,6,30,31]</sup>

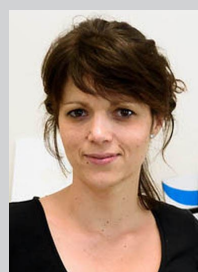
The formation of lead and zinc soaps occurs due to the presence of lead and zinc-based compounds, such as lead white (basic lead carbonate,  $2\text{PbCO}_3 \cdot \text{Pb}(\text{OH})_2$ ) and zinc white (zinc oxide,  $\text{ZnO}$ ), in oil paint systems both in painted layers and/or in the ground.<sup>[32]</sup>

It was observed that lead soaps are almost always associated with protrusions, (i.e., whitish or opalescent circular lumps characterised by crater-like edges as a result of a pressure towards the painted surface), crusts, efflorescence hazes and increased transparency.<sup>[1]</sup> A study by Cotte et al. highlighted that lead-based compounds used as driers (e.g., lead oxide) and not as pigments, might be the main responsible for the protrusions formation.<sup>[33]</sup> The formation of the new compounds in the system produces an expansion of the volume that may exert a pressure leading to a mechanical expansion. One of the most dangerous and worst consequences could be the formation of cracks in the paint surface and, finally, paint losses or *lacunae*.<sup>[3,4,7,22,34,35]</sup>

On the other hand, it was observed that zinc soaps are associated with different degradation problems than lead soaps. In particular, they can compromise the mechanical proprieties of paintings through delamination, flaking and

cleavage of the films.<sup>[1,17,19,20,36–39]</sup> Zinc soaps are considered quite dangerous and invasive for paintings and their nature and behaviour have received significant attention.<sup>[17,40,41]</sup> Nevertheless, it is not clear why delamination is caused.<sup>[36]</sup> Rogala and co-workers observed that together with zinc white, a significant but unusual concentration of unsaturated fatty acids, and particularly oleic acid, was detected in the organic fraction of samples using chromatographic/mass spectrometric techniques; this led Rogala et al. to suggest that  $\text{ZnO}$  forms a packed crystalline structure which “traps” the carbonic chains of oleic acid and hinders their cross-linking. This mechanism could explain the structural instability and the formation of an unusually stiff and brittle paint layers where typical plate-like cleavage, delamination, and cracks may occur, with important conservation consequences.<sup>[38,42]</sup> It is noteworthy that zinc white-containing layers were found to have different mechanical behaviour compared to lead white. Studies carried out on grounds made up of basic lead carbonates have shown a higher elasticity than zinc grounds.<sup>[29,38,43]</sup>

Metal soaps are not always harmful and are important additives in manufactured paint formulations. Since 1920, metal stearates, especially zinc and aluminium stearates, were often added to commercial artist oil paint as dispersion agents.<sup>[22,36,43,44]</sup> They prevent the separation of the pigment from the oil, help the pigments to disperse inside the medium and stabilize the pigment itself therefore, the amount of oil is progressively reduced.<sup>[12,13,36]</sup> They may be a supplementary source of free fatty acids within a paint system,<sup>[37,45,46]</sup> but their impact on additional metal soaps formation is unknown.



Francesca Caterina Izzo is an Assistant Professor in Conservation and Heritage Science at Ca' Foscari University of Venice (Italy). She coordinates the group of the Italian Society of Chemistry devoted to “Diagnostics for Cultural Heritage”. Her research focuses on painting materials, modern and contemporary oil paints, the assessment of new analytical methods and protocols for conservation.



Matilde Kratter graduated in 2020 at Ca' Foscari University of Venice (Italy) in Conservation Science and Technology for cultural heritage with a master thesis entitled “An insight into ion migration process in commercial oil paint systems” focused on metal soaps formation in contemporary paintings. Currently, she has a scholarship at Ca' Foscari University.



Austin Nevin is a Reader and the Head of Conservation at the Courtauld Institute of Art, London. His research focuses on the development and application of analytical techniques for studying easel paintings and wall paintings, that includes the identification of materials, as well as the assessment of the condition and conservation of works of art.



Elisabetta Zendri is an Associate Professor in Conservation and Heritage Science at Ca' Foscari University of Venice (Italy), where she leads the research group “Chemical Sciences for Cultural Heritage”. She is the coordinator of the Master's degree in Conservation Science and Technology for Cultural Heritage. Among her research activities, she is involved in the investigation and conservation protocols for modern and contemporary oil paintings.

This review is organized in three main sections. The first section provides a brief and general description of the most up to date theories regarding the chemical and physical processes involved in the formation of metal soaps. The second section illustrates the most commonly used analytical techniques for the identification, localisation and study of metal soaps in oil paintings and paint samples.

## 2. Composition, Formation and Migration of Metal Soaps in Oil Paintings

Metal soaps are a broad class of chemical compounds that are metal carboxylate salts, characterized by the general formula  $M(\text{RCOO})_n$ , with R a long-chain fatty acid.<sup>[22,39]</sup>

Currently, it is believed that the formation of metal soaps in oil paintings is due to the composition of paint, the drying of oils and the ageing of oil paint films.<sup>[39]</sup>

Exhaustive studies by Hermans et al., conducted in the past five years, have contributed to have a detailed knowledge of the processes that lead to metal soaps formation.<sup>[39,47–51]</sup> Indeed, the ageing of oil paint films and the formation of metal soaps films is influenced by extrinsic and intrinsic factors.<sup>[17,52,53]</sup> The intrinsic factors are related to processes that occur at the interface between pigment and drying oil, while the extrinsic ones are related to environmental or anthropogenic causes (i.e. Relative Humidity – RH – and Temperature or restoration treatments).<sup>[17,22,52,53]</sup> The complexity of the phenomena involved in oil paint ageing and the formation of metal soaps continue to engage experts in heritage science.

### 2.1. Chemical Nature and Drying of Oil

The traditional drying oils (such as linseed, poppyseed and walnut oils) used in oil painting are mixtures of triglycerides (TAGs) with a high percentage of mono-, di- and tri-unsaturated octadecanoic acids (namely respectively (9Z)-Octadec-9-enoic acid, (9Z,12Z)-octadeca-9,12-dienoic acid, (9Z,12Z,15Z)-octadeca-9,12,15-trienoic acid, also known as oleic, linoleic and linolenic acid). The drying process of these oils occurs through a series of autoxidation processes, i.e. the spontaneous reaction of the C=C bonds in the unsaturated fatty acids with the oxygen present in the atmosphere.<sup>[52]</sup> Oxidation is followed by polymerization and the formation of a densely cross-linked molecular network. After autoxidation processes occurred, radicals and subsequently peroxides are formed. These reactive radicals successively reacts with other compounds present in the system leading to the formation of secondary (aldehydes, ketones and alcohols) and tertiary (dicarboxylic acids) products.<sup>[52,53]</sup> After autoxidation processes occur, spontaneous hydrolysis of the ester bonds of the TAGs may cause the “release” of fatty acids as free saturated fatty acids (SFAs, R-COOH).<sup>[7,54]</sup> Free SFAs are also produced after the hydrolysis of TAGs.

It was observed that carboxylic acid functionalities are able to adsorb on metal oxide, such for example zinc white (ZnO).<sup>[17,39,55]</sup> Artesani suggests that different configurations are possible and that they depend on the type of metal oxide. In the case of zinc white, the surface of pigment is progressively functionalized by free SFAs, thanks to ion-covalent bonds formation: van der Waals forces contribute to the bonds between polar carboxylates and the pigment.<sup>[17]</sup>

When ZnO is present in oil, the favoured binding mode between carboxyl groups and zinc atoms is dissociative bridging adsorption: carboxyl groups attach to two Zn atoms and the dissociated hydrogen bonds to another Zn atom.<sup>[17]</sup> Significant forces act in the lateral chain-chain interactions thus the energy of adsorption decreases with increasing fatty acid chain length.<sup>[17,39]</sup> Carboxylic-metal surface interactions are expected to be a common phenomenon for many pigments in polymerized linseed oil.<sup>[55]</sup>

### 2.2. Ionomer Formation

Once carboxylic-metal interactions develop in the paint system, metal cations can spontaneously migrate into the polymerised network, moving from one carboxylate group to another and, when many free carboxylate groups in the binding medium are bound to a metal ion, a ionomer-like structure (i.e. a polymer containing cross-links formed by ionic groups neutralised by metal cations) is formed.<sup>[17,39]</sup> It is, therefore, necessary that bound and unbound carboxylic groups are in proximity, and polymer segments are mobile.<sup>[39]</sup> External factors (such as solvents in conservation treatments) may modify the mobility of binding media and the diffusion rate<sup>[56]</sup> of the metal with two consequences: the leaching of metal ions from pigments and the possibility that metal soaps can form anywhere.<sup>[39]</sup> Despite mobility of ions, the ionomeric system leads to an increase in the stiffness of the binding medium since divalent ions may coordinate two carboxylates to balance their charge, thus reinforcing the ionomer network.<sup>[55]</sup> Ionomer networks are stable and no transfer of metal ions is expected if all carboxylates functionalities are bound to metal ions.<sup>[39]</sup>

### 2.3. Hydrolysis Process

Hydrolysis of the lipidic binder leads to the formation of new free SFAs and this process is gradual.<sup>[52]</sup> Ester groups of TAGs can react with water molecules, forming carboxylic acids group and alcohol groups.<sup>[39,52]</sup> Some cations, such as,  $\text{Pb}^{2+}$  and  $\text{Zn}^{2+}$ , play an important role in hydrolysis, since they act as Lewis acids and contribute to the destabilization of the CO bond of ester groups of TAGs. Van Loon et al. observed that, hydrolysis occurs often close to the pigment surface, where metal ions are available.<sup>[57]</sup>

In manufactured oil paints, aluminium stearates (commonly added as dispersion agents) may increase not only the saturated fatty acid content but also decrease the stability of the CO bond since  $\text{Al}^{3+}$  is a strong Lewis acid.<sup>[12,30,39,53,58]</sup>

The direct impact of RH on the formation of metal carboxylates suggests that water may affect not only the rate of triglyceride hydrolysis, but also the mobility of metal ions. Other environmental factors, such as light and temperature, may influence these phenomena.<sup>[16,59,60]</sup>

It was also observed that restoration campaigns which involve solvent-based operations and thermal treatments, can plasticize the medium allowing a higher mobility of free SFAs.<sup>[17,56]</sup> Hydrolysis leads to the variable transition from an ionomeric structure to mixture of free SFAs and metal ions.<sup>[39]</sup> The metal ion-carboxylate group complexes can react with other carboxylate functionalities, released by hydrolysis (as illustrated in Figure 1A/B), and once the binding medium becomes supersaturated with metal soaps and is metastable, spontaneous crystallisation of soaps can occur.

## 2.4. Crystallisation of Metal Soaps

As reported in References [17,39], the exact mechanism and factors that control the rate of growth of metal soap crystals are not yet completely elucidated. For the formation of a crystalline nucleus generated from metal soaps, it is necessary to overcome the energy threshold represented by the maximisation of Van der Waals interaction. To this aim, the alignment of alkyl chains occurs.<sup>[17,39]</sup> The rate of crystallisation has been qualitatively measured by Hermans et al.: they observed that lead and zinc palmitate in linseed oil crystallise at circa 50 °C and 6–9 °C below their melting point, respectively. These two different temperatures underline that, in the case of a fully polymerized binding medium, zinc soaps may be kinetically trapped in an amorphous state, while lead soaps could crystallise rapidly.<sup>[39]</sup>

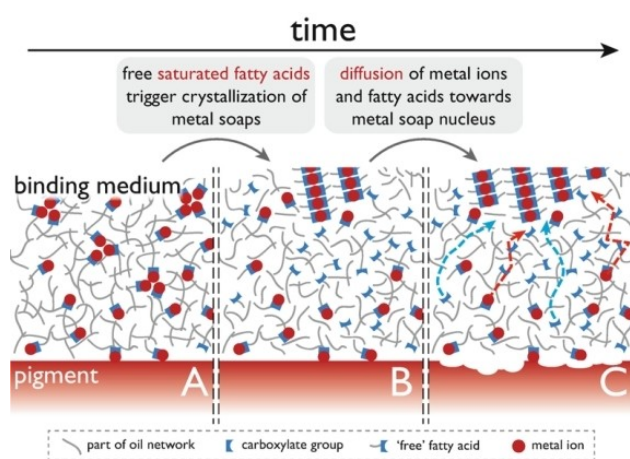


**Figure 1.** Illustration of metal soap-related degradation processes in an ionomeric binding media (a), triggered by the presence of free SFAs (b) and resulting in the formation of large crystalline metal soap phases (c). Dashed arrows illustrate the diffusion of metal ions (red) and free SFAs (blue) toward the growing crystalline metal soaps aggregate. Reproduced from the PhD thesis “Metal Soaps in Oil Paint. Structure, Mechanisms and Dynamics” - University of Amsterdam, 2017 with permission from J. J. Hermans (copyright holder) from the PhD thesis “Metal Soaps in Oil Paint. Structure, Mechanisms and Dynamics” - University of Amsterdam, Faculty of Science (FNWI), Van't Hoff Institute for Molecular Sciences (HIMS), 2017.

Once nucleation occurs, the growth of crystals of metals soaps follows. When metal ions and fatty acids decrease their concentrations in proximity to crystalline metal soaps, it was observed that other fatty acids and metal ions from the binding medium move toward the crystalline phase due to a concentration gradient (Figure 1C).<sup>[39]</sup> This last step can be considered as the starting point of degradation of paint, since fatty acids have been released from the binding medium and metal ions have dissolved from pigments, driers and/or additives.

The abovementioned phases are characterized by different time scales.<sup>[17,33]</sup> For example, in the case of zinc oxide, it was observed that although zinc complexes form rapidly metal soaps formation is slow.<sup>[17]</sup> On the other hand, Cotte et al. observed that in model mixtures and in a facsimile of an ancient painting, the formation and crystallisation of lead soaps occurred just after a few weeks.<sup>[33]</sup> The most evident defects in lead paints have been detected after ageing: this suggests that the formation of aggregates occurs during the mature ionomeric phase of the paints rather than during the drying of oil.<sup>[34]</sup>

## 2.5. Why Should We Study Metal Soaps?

Studies on metal soaps are constantly developing and are aimed at better understanding several aspects of their evolution. In particular, conservation practice needs to develop new and suitable measures for facing and addressing potential degradation processes related to metal soaps.<sup>[62]</sup> Research suggests that the timely recognition of the metal soaps presence plays a fundamental role in the preservation of artworks.<sup>[17,39,62]</sup> The most effective measure to prevent metal soap formation and the mitigation of their appearance is by detecting metal soaps at their early formation stage, without affecting the integrity of the paint film.<sup>[17,39,62]</sup> At the same time, it is recognised that metal soaps do not always represent a hazard for the conservation of artworks. Indeed, metal soaps sometimes play a positive role in the polymeric network even acting as a sort of anchor points for the carboxylic acid groups during paint drying processes, promoting self-repair mechanisms and reducing the swelling of the paint film.<sup>[22]</sup> Thus metal soaps may be considered a type of stabilizer which is an important consideration if they are removed during cleaning.<sup>[7,22,34]</sup>

## 3. How to Detect Metal Soaps

There are multiple analytical techniques and methods that have been adopted in the study of metal soaps. In this review, a selection of the most commonly applied techniques to identify, localise and study metal soaps is presented: Optical Microscopy (OM), Photoluminescence (PL) spectroscopy and imaging, Scanning Electron Microscopy in Back Scattered Electron mode (SEM-BSE) or with Energy Dispersive X-ray spectroscopy (SEM-EDX), Secondary Ion Mass Spectrometry (SIMS), Fourier Transform Infrared (FTIR) and Raman spectroscopy, X-ray diffraction

(XRD), Nuclear Magnetic Resonance (NMR) and Gas Chromatography-Mass Spectrometry (GC-MS). These methods are critically reviewed, underlining advantages and drawbacks in their application on the study of metal soaps.

References reported in the following paragraph referring both to metal soap-samples that have been synthesised in the laboratory and metal soaps from paintings.

Analysis provides information about the composition, the morphology and the distribution of metal soaps. Results obtained from model samples are fundamental for interpreting complex issues related to the mechanisms of soap formation and migration. In fact, the characterization of model paint samples prepared under controlled conditions with varying paint compositions (including different pigments, pigment-to-oil ratios and additives) allows the controlled study of the effect of paint ingredients on metal soap formation.<sup>[35,49,51,55,58,63–65]</sup>

### 3.1. Optical Microscopy (OM)

The identification of metal soaps can be made by carefully observing the surface of paintings, as reported by Noble and Boon (see 1. Introduction). As highlighted in Figure 2, protrusions related to metal soap formation have created a pitted painted surface, easily visible by Optical Microscopy (OM) and sometimes even with the naked eye.

An optical microscope is a powerful tool for the detection of metal soaps on paint surfaces and in cross-sections. Lead and zinc soaps, observed by OM, appear as transparent or whitish opaque masses, characterised by a circular form with a diameter ranging from 10 to 200  $\mu\text{m}$ , and may grow up to 500  $\mu\text{m}$  or even larger.<sup>[4,6,14,66,67]</sup> White lumps or inclusions are often visible on the surface of the paintings, mainly in films containing lead white or lead-tin yellow type I.<sup>[14,67]</sup> The aggregates may remain small dimensions or may increase in size. The latter, since they lead to a volume expansion, later can break through the



**Figure 2.** Nicolaes Berchem, (1620–1683), *Allegory of Summer*, ca. 1680, Mauritshuis, inv. no. 1091, canvas, 94 cm  $\times$  88 cm. Overall (inset), and detail from (red) drapery of standing figure (left of centre) where aggregates have broken through two layers of relatively recent overpaint. Reproduced from “Chemical changes in old master paintings II: darkening due to increased transparency as a result of metal soap formation” with permission from Petria Noble (copyright holder).

overlying layers and protrude on the surface.<sup>[7]</sup> As a result of mechanical stress, fractures and delaminations, even flaking of paint can be observed.<sup>[23,37]</sup> In van Gogh’s masterpiece *Roses* (1890), for instance, a chalky appearance was observed together with small fissures aligned with the fibres of canvas.<sup>[18,68]</sup>

Sometimes, the damage due to metal soaps have been observed as dark spots. This appearance is likely due to conservation treatments more than saponification itself. Once protrusions have erupted on the surface, they were often removed or abraded by treatments carried out during conservation. The holes created have over time become darker spots due to the accumulation of dirt and the pooling of aged varnishes and coatings layers, resulting in a pustule-like appearance on the surface.<sup>[4]</sup>

OM is essential for the observation of paint cross-sections, allowing the detection of aggregates of metal soaps in paint layers,<sup>[6,69]</sup> and to determine how many layers are affected by the phenomenon and to assess differences between the aggregates and the surrounding particles.<sup>[6]</sup> The examination of cross-sections often suggests that lead and zinc crystalline soaps aggregate and collect in preferential locations: lead soaps tend to form close to the interface between paint layers, while zinc soaps may form towards the bottom of zinc white paint layers.<sup>[17,39,70]</sup> This type of spatially different development could be due to a variety of factors that affect either the nucleation or the growth of crystals.<sup>[39]</sup>

Small orange particles have also been observed in cross-sections when red lead (i.e. minium) and lead soaps are detected.<sup>[4,34,70,71]</sup> Once lead soaps have crystallised and highly alkaline conditions are present ( $\text{pH} > 12$ ), they may undergo mineralisation in addition to aggregation with new the development of new mineral compounds such as carbonates, chlorides, oxides and sulfates of metal cations present in pigments.<sup>[4,10,34,70]</sup> The presence of a whitish centre (the soap) and orange compounds (secondary products), distributed in some regions of the paint stratigraphy, have led scientists to suggest that mineralisation of lead soaps may occur. This phenomenon is important since it underlines the early stage of development of aggregates and their progressive conversion into new mineral phases.<sup>[70]</sup>

With low cost and immediate legibility of paint layers, OM is perhaps the most important technique for the study of paint stratigraphy but relies on expertise in sample preparation and experience for the interpretation of micrographs. The main drawback of OM is its low chemical specificity.<sup>[72]</sup>

### 3.2. Ultraviolet Radiation and Photoluminescence-Based Techniques

Cultural heritage materials are often luminescent.<sup>[73]</sup> Although organic materials are generally characterized by broad emissions, and their luminescence is not considered as diagnostic, other paint components, including semi-conductor pigments like ZnO, are characterized by defined and strong luminescence.<sup>[74]</sup>

Photoluminescence (PL) represents a qualitative and non-destructive technique that can improve the differentiation of materials in paint cross-sections.<sup>[72]</sup> PL properties of a material should be related to synthesis and impurities and may be a consequence of degradation and chemical reactions (complexation).<sup>[75]</sup> Although PL can provide key information regarding degradation of materials, past interventions and phases of metal soaps,<sup>[72,73]</sup> it is generally employed as an auxiliary technique for examining samples.<sup>[18]</sup>

Several studies have reported ultraviolet (UV) radiation, in particular UV-A, to better observe zinc and lead soaps in cross-sections since paint layers may exhibit heterogeneous luminescence.<sup>[4,18,67,72]</sup>

The fluorescence observed from lead aggregates may vary, allowing the distinction between lead aggregates and ordinary coarse particles of pigments (such as lead white).<sup>[67]</sup> Furthermore, it was observed that lead white shows different luminescence in the initial saponification processes and after the formation of soap aggregates.<sup>[18]</sup>

On the other hand, Zinc oxide is a fluorescent pigment by itself (it belongs to the class of II–VI semiconductors) and has two main crystalline forms. The hexagonal structure (the most stable, thereby the most common) has a band gap energy of 368 nm at room temperature, while the cubic structure has a lower absorption edge energy (459 nm).<sup>[76]</sup> ZnO exhibits two characteristic optical emissions: the direct band-to-band recombination (BE), that produces a narrow emission at 380 nm, and the trap state levels (TS), with the most intense emission being centred in the visible spectral region (around 530 nm). TS emissions are caused by intrinsic defects and impurities in the crystal structure and recent studies have hypothesised that the most common TS emission, centred at 520 nm, is due to extrinsic defects incorporated in synthesis processes.<sup>[76–80]</sup> This univocal characteristic discriminates defects and/or impurities in zinc oxide crystals, since they emit at longer wavelengths.<sup>[73,78]</sup> In addition, heterogeneity in photoluminescence is used to discriminate among different batches of zinc white, and consequently between the different pigment production processes.<sup>[72,74,81,82]</sup>

Salvant and co-workers applied imaging photometric stereo (PS) acquisition under UV radiation to non-invasively characterise the 2D-distribution and occurrence of metal soaps protrusions on the surface of the painting *Pedernal* (1941) by G. O'Keeffe.<sup>[14]</sup> The main results obtained on the micro-scale correlated the uneven distribution of protrusions to the paint composition and not to the priming layers, as was supposed in the past. In addition, the profiles of size distributions are overall similar for the different coloured areas, with a dominant proportion of protrusions in the 100–200  $\mu\text{m}$  range.<sup>[14]</sup>

The dynamics of the luminescence emission can provide insights on metal soaps using PL imaging and spectroscopy techniques. A recent example is provided in research by Thoury and co-workers, who adopted a synchrotron photoluminescence imaging technique, implemented with deep-UV radiation (SR-DUV-PL) to obtain information about lead and zinc soaps at submicron scale.<sup>[18]</sup> They observed the structure and the morphology of metal soap alteration products during their early

stages of formation and when soaps were present as large aggregates. Considering that unaltered lead white does not show any detectable luminescence in the UV range adopted, the data obtained suggested that lead soaps formation and chemical changes occurred at the edges of the pigment particles: in fact, the upper and lower edges of lead particles were characterized by strong luminescence.<sup>[18,58]</sup> To distinguish even more clearly between the different aggregate phases, a false-colour photoluminescence emission with a specific set-up was developed.<sup>[18]</sup> Moreover, Thoury and co-workers adopted UV-C excitation and false-colour multispectral imaging to visualize the zinc soaps phases that are present in *Roses* by Vincent Van Gogh (1890). Van Loon et al. employed SR-DUV-PL to distinguish between zinc white and zinc soaps present in paint layers, thanks to different emission filters ranging from 327 to 870 nm.<sup>[19]</sup> In particular, the 370–410 nm emission image was used to map the presence of zinc white,<sup>[78]</sup> while the 327–353 nm emission image was used to map zinc soaps.<sup>[18]</sup>

To overcome the limitations related to the strong luminescence of zinc oxide, Hageraats and co-workers employed a deep-UV excitation and UV emission lower than 375 nm and were able to identify weak luminescence from samples with zinc soaps.<sup>[20]</sup> This methodology is powerful for the examination of paint samples since the lateral resolution of the instruments is diffraction-limited for emission wavelengths down to 400 nm.<sup>[72]</sup> A recent example of SR-DUV-PL applications is the analysis of cross-sections from *Composition with Color Planes 4* by Piet Mondrian (1917) where four types of ZnO particle were identified, based on their luminescence.<sup>[72]</sup> In addition, the photoluminescence signal measured on a sample in the 327–353 nm emission range originate from crystalline zinc soaps. This conclusion was reached thanks to a high spatial correlation with a  $\mu\text{-ATR-FTIR}$  map of zinc soaps and a semiquantitative analysis of the photoluminescence behaviour of zinc palmitate and other aged paint components.<sup>[72]</sup>

Artesani and co-authors investigated zinc white (and corresponding metal soaps) by time-resolved photoluminescence (TRPL) spectroscopy.<sup>[76,83]</sup> This technique is based on the measurement of the temporal properties of fluorescent emissions with picosecond and nanosecond temporal resolution, can distinguish between BE and TS emissions of zinc oxide.<sup>[77,79,81,83]</sup> The lifetimes of the different PL emissions and the dependence of the PL emission intensity with respect to the fluence is important as this will impact the observed colour of ZnO in paint cross sections.<sup>[76]</sup> During curing and ageing of ZnO-based paint films, photoluminescence behaviour of zinc white changes: these modifications are ascribed to the adsorption of carboxyl and hydroxyl groups and the formation of bonds on pigment particle surfaces and, thus, influenced by the presence of zinc carboxylates.<sup>[76,83]</sup>

UV and laser-based photoluminescence techniques are efficient in the investigation of metal soaps, but the interpretation of data is not straightforward. The presence of UV absorbers can severely influence the fluorescence signal and distort recorded spectral features (i.e. colours in the painted layer can strongly modify the emission from organic binders). Secondly, the spatial distribution and intensity (illuminance) of

the excitation light (typically uneven) and lighting can affect measurements.<sup>[18,73]</sup>

### 3.3. Scanning Electron Microscopy in Back Scattered Electron Mode and with Energy Dispersive X-Ray Spectroscopy (SEM-BSE and SEM-EDX)

Scanning Electron Microscopy in Back Scattered Electron mode (SEM-BSE) and/or with Energy Dispersive X-ray spectroscopy (SEM-EDX) is essential to observe, detect and identify metal soaps and their morphology on the nano-scale in oil paintings. The main advantages are the high magnification and the possibility to obtain information regarding both the internal morphological structure of aggregates (through SEM-BSE) and the elemental identification of the distribution metal cations (through EDX) involved in the saponification and mineralization processes.<sup>[84,85]</sup>

In the case of lead soaps, the inhomogeneity clearly visible when aggregates and analysed with UV radiation is more appreciable through SEM analysis. Lead soaps are characterized by highly scattering and less scattering regions: the first ones are correlated to lead-rich areas and are surrounded by the latter ones, which correspond to more UV-fluorescent regions. In addition, lead-rich areas present a lamellar structure, mostly towards the centre of the inclusions.<sup>[67]</sup>

The emblematic case of lead soap formation in the painting *The Anatomy Lesson* (1632) of Dr Nicolaes Tulp by Rembrandt van Rijn was studied through a multi-analytical approach by Keune and Boon.<sup>[84]</sup> BSE and elemental mapping by EDX revealed that the distribution of binding medium and metal soaps is heterogenous throughout the cross-sections and within the same layer. The authors identified a flesh-toned paint layer which was partially saponified and with a relatively high pigment/binder ratio. In addition, only the lower part was found to be affected by lead soap formation. Therefore, Keune and Boon hypothesized that lead white paint layers could have reacted with fatty acids to form metal soaps, thereby metal soap formation is not limited to a single layer nor dependent on the granularity of the lead white.<sup>[84]</sup> The analytical imaging studies applied on paint cross-sections elucidated the processes involved in lead soap aggregation and mineralization.<sup>[84]</sup> BSE images show that saponified areas appear darker than the unsaponified lead white areas, due to their higher organic content.<sup>[57]</sup> Moreover, BSE images depicted a different scattering between mineralized areas of paintings and the new mineral phases, where the scattering is more attenuated.<sup>[85]</sup>

Platania and co-workers investigated the aging processes and consequently the metal soaps formation, in two paint samples. They come from a late-medieval wing panel painting from an altarpiece in the church of Skjervøy (Troms).<sup>[70]</sup> Figure 3 illustrates the lead-based pigment dissolution that occurred in the less scattering regions, in contrast with highly scattering areas which, instead, corresponds to not-degraded pigment particles. In addition, the typical striations due to metal soaps aggregates were not observed suggesting the presence of single dispersed metal soap precipitates.<sup>[70,85]</sup>

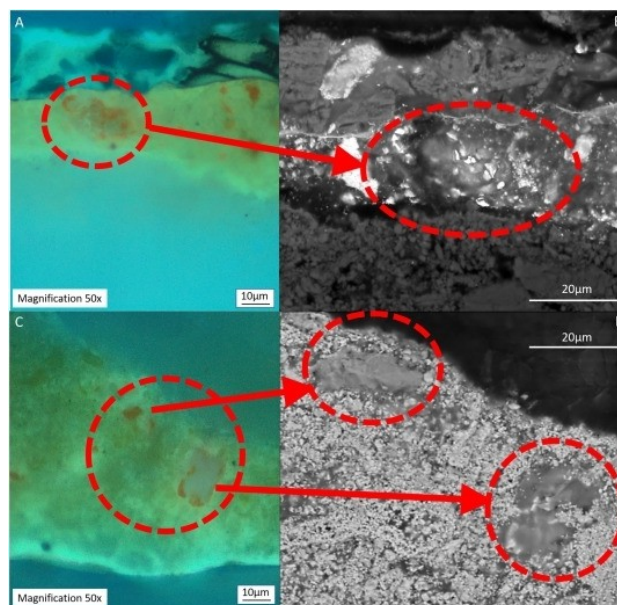


**Figure 3.** Details of the mineralized regions when observed under UV light (magnification 50 $\times$ ), cross-sections L175\_9 (A) and L175\_6 (C). BSE images of mineralized lead soap regions of cross-sections L175\_9 (B) and L175\_6 (D). Reproduced, with permission from reference.<sup>[70]</sup> This Agreement between Dr. Francesca Caterina Izzo ("You") and Elsevier ("Elsevier") consists of your license details and the terms and conditions provided by Elsevier and Copyright Clearance Center.

BSE images of ZnO-based painted layers, obtained by Osmond and co-workers, were useful to assess zinc oxide particles: they observed not only that particles characterized by smaller and nodular form react before larger or acicular ones, but also that zinc oxide particles react more readily than lithopone ( $\text{ZnS}-\text{BaSO}_4$ ), lead white and coloured pigments.<sup>[36,41,68,86]</sup> Moreover, the observations of BSE images show that the early-stage saponification of zinc oxide is characterized by zinc-based regions with poorly defined boundaries, relatively low pigment density and reduced atomic brightness. In this way, it was possible to differentiate metal soaps that form from reactions between ZnO and oil medium from original components (additives). Osmond stated that additives are commonly characterized by discrete particle-free areas with clear boundaries.<sup>[36]</sup>

An example of BSE images from a paint sample from *Untitled (Ploughing)* by E. Philips Fox (1989) revealed an unusual morphology in correspondence of zinc white paint layer. Since no small nodular zinc oxide particles were observed, Osmond suggested a mechanism of formation of zinc soaps: zinc oxide particles have reacted elsewhere, leaving an amorphous zone containing dispersed acicular zinc oxide particles, surrounded by zinc carboxylates.<sup>[36]</sup>

More recently, Hermans and co-workers employed SEM to obtain three-dimensional tomographic reconstructions to explore the first stages of disfiguring formation of zinc soaps occurring in modern oil paintings.<sup>[64]</sup> SEM images show that the soap is composed of many small (semi-) crystalline domains, each with a coordinated layered structure of 50–100 nm size,



without a specific orientation. Zinc plates are organized in successive layers and are separated by lipidic polymers forming a 3D flower-like-structure. These “flowers” are related to the initial precipitation of zinc soaps. Moreover, the distribution of these domains are quite homogeneous and uncorrelated to location of ZnO particles confirming the hypothesis that nucleation processes occur in the binding medium and not on pigment particles.<sup>[17,39,49,64]</sup> This finding suggests that zinc soaps may be present both as amorphous zinc carboxylates, bound to the oxidized, cross-linked oil network, and as crystalline zinc soaps, which are most frequently linked to paint degradation.<sup>[36,49,50,87]</sup>

Romano and co-workers studied irregularly shaped protrusion of zinc soaps both in top view and in cross-sections. These eruptions are present on the surface of test panel paint and are translucent and gel-like.<sup>[87]</sup> Using SEM-EDX analysis, authors were able to detect a Zn concentration gradient in the samples. A uniform distribution of Zn was detected using surface observation, while in the cross sections Zn is more present in the edges of the gel than in the centre. This implies that the centre of the gel material has not reacted to form zinc carboxylates to the same extent as the outer edges of the gel. The zinc carboxylate concentration gradient provides some indications of the mechanisms involved in zinc carboxylates formation and migration. The saponification appeared to be in a relatively early stage, despite some apparent degree of crystallinity determined by ATR-FTIR.<sup>[87]</sup>

SEM techniques are characterized by some technical limitations: spatial and depth resolution of about 1–5 nm and 10–1000 nm respectively; the detection limit of EDX is about 0.1 wt% for pure materials; the quality of the BSE images depending on the surface roughness; the detection of light elements is limited when they are present in low concentrations. Despite these limitations, we believe that the use of SEM is fundamental for the continued study of metal soaps.<sup>[6,70,72,87]</sup>

### 3.4. Vibrational Spectroscopic Techniques

Much of the literature on metal soaps analysis is based on the application of spectroscopic techniques, such as FTIR and Raman Spectroscopy. FTIR and Raman spectroscopies have been widely adopted in Heritage and Conservation Science: both techniques can be used directly in situ and in a non-invasive way and to analyse samples on the micro scale and on cross-sections.<sup>[8,10,34,66,88,89]</sup> Analytical investigations using FTIR and Raman spectroscopies were first carried out on “pure” metal soaps synthesized in laboratory. Exhaustive work by Robinet and Corbeil provided precious information that gave an initial overview of the spectroscopic properties of metal soaps.<sup>[44]</sup>

Discrepancies may arise when comparing lab-produced mock-ups with real case studies: the wavelengths of absorbance of scattering may vary because of the simultaneous presence of more fatty acids, both saturated and unsaturated,<sup>[39,90]</sup> the environment conditions<sup>[69]</sup> and/or an incomplete crystallisation

of aggregates.<sup>[39]</sup> Despite the many drawbacks, model systems are essential to understand the link between molecular structure or composition and paint degradation<sup>[91]</sup>

### 3.5. Fourier Transform Infrared Spectroscopy (FTIR)

Use of FTIR for the analysis of metal soaps, both as standard materials<sup>[26,44,92,93]</sup> and from real case studies is widespread.<sup>[9,13,33,50,59,69,74,89,94–96]</sup> Many studies have demonstrated how IR spectroscopy can provide essential information both regarding the behaviour of metal ions in oil paint and their surrounding molecular environment.<sup>[91]</sup>

Detailed knowledge has been gained regarding both the common (lead and zinc) and the less common (copper, cadmium, calcium, cobalt, gallium, iron, tin and manganese) metal ions that react with different fatty acids such as azelaic, stearic, palmitic and oleic acids.<sup>[26,44,92,93]</sup> Table 1 summarises the most characteristics IR absorptions of synthesized metal soaps.

Metal soaps share similarities with molecules of siccative oils: both, in fact, are characterised by carboxylic groups (RCOO<sup>-</sup>) and carbon chains (CH<sub>2</sub>, CH<sub>3</sub>). The presence of cations in metal soaps causes a shift of the typical siccative oil absorptions related to COO<sup>-</sup> which normally falls between 1750 and 1730 cm<sup>-1</sup>.<sup>[97]</sup> When a metal soap is formed in a drying oil matrix, two important modifications of the vibrations from molecules in siccative oil occur:<sup>[44,98]</sup>

- the decrease of the intensity of the broad band in the region between 3300 to 2500 cm<sup>-1</sup> attributed to the O–H stretch;
- formation of a sharp absorption attributed to the  $\nu_{as}$  and  $\nu_s$  of COO<sup>-</sup> between 1550 and 1400 cm<sup>-1</sup>, due to the replacement of the bands assigned to the C=O and C–O that between 1700 and 1300 cm<sup>-1</sup>.

The position of the carboxylate absorption is related to the metal present in the soap, while the weaker absorption at 1300–1100 cm<sup>-1</sup> can be used to discriminate the fatty acid in soaps.<sup>[44]</sup> The region of the IR spectrum between 1800 and 650 cm<sup>-1</sup> is generally considered and discussed by researchers since the CH stretching profiles are not subject to significant modification. In this region, the area between 1600 and 1400 cm<sup>-1</sup> is important: here, the asymmetric and symmetric stretching bands of COO<sup>-</sup> occur and it is possible to discriminate different metal ions of a specific carbon chain.<sup>[92]</sup> The data reported above refer to synthesised metal soaps which differ from metal soaps detectable in real artworks since they are pure and not in mixtures with other substances. In paintings metal soaps are present in low concentrations, which may limit their analysis by FTIR since its detection limit is estimated to be around 5% (in weight) in a mixture.<sup>[97]</sup>

It has been observed that the FTIR spectra of zinc soaps were often different from the corresponding zinc carboxylates reported in literature. Recent studies have demonstrated that, since zinc soaps are part of network-coordinated systems, their carboxylate moieties are covalently bound to the cross-linked and cured oil matrix.<sup>[17,39,48,50,55,98]</sup> Several examples shows this characteristic, especially for zinc.<sup>[9,64,99]</sup> In addition, the signals in paint samples can vary because of the simultaneous presence

**Table 1.** In the following table the most characteristics IR absorptions are reported in the range between 1800–650 cm<sup>-1</sup>.<sup>[26,44,92,93]</sup> The bands that allow distinction between the different carbon chain lengths are highlighted in bold.

	Palmitate	Stearate	Oleate	Azelate	Assignment
Lead	1540–1538 sh <b>1508–1513 s</b>	1541–1538 sh <b>1513 s</b>	1504 sh, <b>1488 s</b>	<b>1513 vs</b>	$\nu_{as}[\text{COO}^-]$
	1461 m	1473–1461 m	1471 sh	1443 sh	$\Delta[\text{CH}_2]$
	1418–1405 m	1420–1418 m	1423 sh, 1405 m	1406 s	$\nu_s[\text{COO}^-]$
Zinc	<b>1539–1536 s</b>	<b>1540–1539 s</b>	<b>1547 vs,</b> <b>1527 vs</b>	<b>1556–1535 vs</b>	$\nu_{as}[\text{COO}^-]$
	1464–1455 m	1465–1464 m	1467 s, 1454 s	1464 s	$\delta[\text{CH}_2]$
	1397 m	1399–1397 m	1407–1404 s	1402 s	$\nu_s[\text{COO}^-]$
Copper	<b>1586 s</b>	<b>1586 s</b>	<b>1588–1584 vs</b>	<b>1588 vs</b>	$\nu_{as}[\text{COO}^-]$
	1468–1444 m	1468–1441 m	1464–1439 w		$\delta[\text{CH}_2]$
	1421 m	1421 m	1433–1426 w	1417 s	$\nu_s[\text{COO}^-]$
Cadmium	<b>1544 s</b>	<b>1544 s</b>		<b>1544 vs</b>	$\nu_{as}[\text{COO}^-]$
	1473–1462 m 1424–1400 m	1463 m			$\delta[\text{CH}_2]$
		1424 m		1424 s	$\nu_s[\text{COO}^-]$
Calcium	<b>1579 s–1540 m-s</b>	<b>1576 –1540 s</b>	<b>1574 –1538 s</b>	<b>1578 vs–1542 vs</b>	$\nu_{as}[\text{COO}^-]$
	1469 m–1434 m	1469 m–1434 m	1468 m	1466 s–1433 sh	$\delta[\text{CH}_2]$
			1431 w	1418 m	$\nu_s[\text{COO}^-]$
Cobalt		1564			$\nu_{as}[\text{COO}^-]$
		1465			$\delta[\text{CH}_2]$
		1432			$\nu_s[\text{COO}^-]$
Gallium		1563			$\nu_{as}[\text{COO}^-]$
		1468			$\delta[\text{CH}_2]$
		1426			$\nu_s[\text{COO}^-]$
Iron		1531			$\nu_{as}[\text{COO}^-]$
		1467			$\delta[\text{CH}_2]$
		1444			$\nu_s[\text{COO}^-]$
Tin		1549			$\nu_{as}[\text{COO}^-]$
		1496			$\delta[\text{CH}_2]$
		1433			$\nu_s[\text{COO}^-]$

Table 1. continued					
	Palmitate	Stearate	Oleate	Azelate	Assignment
Manganese (II)	1569–1564 s	1564–1561 s		1565 vs	$\nu_{as}[\text{COO}^-]$
	1472–1464 m	1468–1466 m		1434 sh	$\delta[\text{CH}_2]$
	1424–1419 m	1438–1419 m		1411 s	$\nu_s[\text{COO}^-]$
Manganese (III)	1568 s, 1545 m				$\nu_{as}[\text{COO}^-]$
	1471 w				$\delta[\text{CH}_2]$
	1430–1404 m				$\nu_s[\text{COO}^-]$

vs = very strong, s = strong, m = medium, w = weak,  $\nu_s$  = symmetric stretching,  $\nu_{as}$  = asymmetric stretching,  $\delta$  = bending.

of more fatty acids, both saturated and unsaturated, the presence of other compounds, both organic (i.e. binders, additives) and inorganic (i.e. carbonates, sulphates, silicates), the impact of environment conditions (humidity) and/or an incomplete crystallisation of aggregates.<sup>[39,69]</sup> Data from FTIR can aid in monitoring the formation of metal soaps in oil systems and in distinguishing the amorphous and crystalline soaps.<sup>[16]</sup> An example is provided by the analysis of the painting "The woodcutter (after Millet)" (1889) by Vincent van Gogh, where different kinds of zinc soaps were identified by Hermans et al. The results highlighted that their IR absorptions differed from standard materials, in particular the asymmetric stretching vibration of  $\text{COO}^-$  is broader and shifted towards higher wavenumbers respect to the absorptions related to metal soaps synthesised and used as references.<sup>[50]</sup> Absorptions with sharp bands are ascribed to the formation of crystalline metal complexes; on the contrary, the broadening and shifting of absorptions are related to amorphous metal carboxylates. As mentioned in Section 2, the formation of an amorphous complex indicates a metal soap not already crystallized and a partially degraded pigment.<sup>[50]</sup>

Only recently, through applications of nonlinear two-dimensional IR (2D-IR) spectroscopy, it was possible to deep the knowledge about the molecular structure of ageing ZnO oil paint.<sup>[55]</sup> Hermans and co-workers stated that the different shapes of the IR band related to zinc carboxylates are associated with variances are the result of the relative concentrations of the oxo- and chains- that the ideal chain complex structure.<sup>[55]</sup> It was observed that both in an ionomer state and in zinc white oil paints, two different species of zinc carboxylates may be present (a tetranuclear oxo- complex and a linear coordination chain complex). After the crystallisation and zinc soaps formation, two different structures may be observed (one that optimizes zinc carboxylate coordination -type A- and one that optimizes fatty acid chain packing -type B).<sup>[55,91,100]</sup> Depending on the nature of fatty acids present in the system, geometry A or B are preferred. The former geometry formed when short-chain, dicarboxylic and unsaturated fatty acids are present while the latter when long-chain saturated often all four types are simultaneously present in a sample, an

overlap of the signals can occur fatty acids are present.<sup>[91]</sup> Beere and co-workers used ATR-FTIR to study oil paint model systems and the influence of parameters (i.e. pigment concentration, carboxylic acid concentration and oil viscosity) in the relative concentration of chain and oxo zinc carboxylate species in oil paint binding media. Moreover, thanks to a computational modelling, they were able to simulate the evolution of these zinc carboxylates during paint drying, aging and under high humidity conditions.<sup>[91]</sup>

The presence of metal soaps in multi-layered paint films can be revealed thanks with micro-FTIR analysis on cross-sections, achieving information on the reactivity of the pigments with the lipid fraction and on the influence of environment conditions.<sup>[34,50,69]</sup> In addition, micro-ATR-FTIR imaging has been adopted in to detect and localise metal soaps, thanks to high chemical specificity and spatial resolution (down to  $\sim 3\text{--}4\ \mu\text{m}$  in the fingerprint region).<sup>[13,26,34,71,101–103]</sup> One of the first applications on lead soaps is by Spring and co-workers at the National Gallery in London.<sup>[103]</sup> Thanks to the introduction of FTIR-imaging, one of the main analytical limits (i.e. the bulk analysis of samples) was overcome since it can identify and localize phases in a region of interest in a non-destructive way.<sup>[104]</sup>

A recent study by Possenti et al. demonstrated that micro-ATR-FTIR spectroscopic imaging can reveal the formation of lead soaps in oil-based paint systems exposed to moisture.<sup>[102]</sup> By combining the qualitative information regarding the spatial distribution of components with the quantitative information from the peak shift in the IR spectra, it is possible to evaluate the degradation of lead white as a function of humidity, the presence of the contiguous organic and inorganic layers and the grain size of lead white.<sup>[102]</sup>

Other FTIR applications for the study of metal soaps involve the use of synchrotron light in combination with micro-FTIR spectroscopy ( $\mu\text{SR-FTIR}$ )<sup>[33,105]</sup> and micro-FTIR spectroscopy combined with X-ray micro-tomography and photothermal induced resonance.<sup>[65,106]</sup> Romano and co-workers performed multivariate analysis on micro-FTIR data from cross-sections characterised by zinc soaps formation. They were able to detect a zinc carboxylate gradient in the cross-sectional view of the gel material, where the edges were rich in zinc carboxylates, and

the centre contained quantities of unreacted linseed oil. This information, together with results from SEM-EDX analysis of the same samples (see SEM-EDX section), provides data about the formation and migration of metal soaps.<sup>[87]</sup>

Despite advantages of FTIR for analysis of model systems, the complexity of IR spectra from real paintings rarely allows the identification of the kinds of fatty acids involved in metal soaps for which other complementary analytical techniques are needed.

Furthermore, when sampling is not allowed or possible (e.g. in the study of miniatures), non-invasive external reflection FTIR spectroscopy (ER-FTIR) may provide information on the composition of surface layers or, eventually, varnishes since the low penetration of IR radiation.<sup>[8]</sup> On the other hand, micro-FTIR based techniques, despite their excellent chemical specificity,

are generally limited to micrometric spatial resolution and cannot give information at the submicrometric scale.<sup>[72]</sup>

### 3.6. Raman Spectroscopy

Raman spectroscopy is often used in the analysis of metal soaps in combination with FTIR, since the two techniques yield complementary data: FTIR gives more reliable information regarding metal cations coordinated to the carboxylate group, while Raman spectroscopy may distinguish the length of the carbon chain.<sup>[44,92]</sup> The characteristic Raman absorptions, in the region between 1200–850 cm<sup>-1</sup>, of the most common metal soaps and fatty acids respectively, are reported in Table 2 and 3.<sup>[44,92]</sup>

**Table 2.** Raman absorptions of synthesized metal soaps in the region between 1200–850 cm<sup>-1</sup>. The bands that allow distinction between the different carbon chain lengths are highlighted in bold.<sup>[44,92]</sup>

	Palmitate	Stearate	Oleate	Azelate	Assignment
Lead	1130 <i>m</i> <b>1100–1099</b> <i>w</i> 1063–1061 <i>m</i>	1131–1127 <i>m</i> <b>1105–1102</b> <i>w</i> 1063–1061 <i>m</i>	1122 <i>w</i> <b>1095</b> <i>m</i> 1062 <i>m</i>	<b>1095</b> <i>s</i> 1064 <i>w</i>	$\nu(\text{C}-\text{C}) + \delta(\text{C}-\text{C}-\text{C})$
	925 <i>w</i>	925–922 <i>w</i>	937 <i>m</i>	942 <i>m</i>	$\rho[\text{CH}_2]$
Zinc	1131–1130 <i>m</i> <b>1101–1107</b> <i>w</i> 1063–1061 <i>m</i> 952–950 <i>w</i>	1131–1129 <i>s</i> <b>1110–1104</b> <i>w</i> 1063–1061 <i>s</i> 952–948 <i>w</i>	1122 <i>w</i> <b>1097</b> <i>m</i> 1065 <i>m</i>	<b>1103</b> <i>s</i> 1064 <i>m</i>	$\nu(\text{C}-\text{C}) + \delta(\text{C}-\text{C}-\text{C})$
			952 <i>w</i>	950 <i>m</i>	$\rho[\text{CH}_2]$
Calcium	1130 <i>m</i> <b>1101</b> <i>w</i> 1062 <i>m</i> 935 <i>w</i>	1131 <i>m</i> <b>1105</b> <i>w</i> 1063 <i>m</i> 932 <i>w</i>		<b>1101</b> <i>s</i> 1064 <i>m</i> 927 <i>m</i>	$\nu(\text{C}-\text{C})$ $\rho[\text{CH}_2]$
Copper	1130 <i>m</i> <b>1098</b> <i>w</i> 1062 <i>m</i>	1130 <i>m</i> <b>1104</b> <i>w</i> 1062 <i>m</i>	1120 <i>w</i> <b>1092</b> <i>m</i> 1064 <i>m-s</i>	1095 <i>s</i> 1062 <i>w</i>	$\nu(\text{C}-\text{C})$
	931 <i>w</i>	937 <i>w</i>	959 <i>w</i>	959 <i>m</i>	$\rho[\text{CH}_2]$
Manganese (II)	1128 <i>m</i> <b>1101–1098</b> <i>w</i> 1062–1060 <i>m</i>	1128 <i>s</i> <b>1103</b> <i>w</i> 1062 <i>s</i>	1120 <i>w</i> <b>1085</b> <i>m</i> 1064 <i>m</i>	<b>1091</b> <i>s</i> 1061 <i>w</i>	$\nu(\text{C}-\text{C}) + \delta(\text{C}-\text{C}-\text{C})$
	946 <i>w</i>	947 <i>w</i>	946 <i>w</i>	947 <i>s</i>	$\rho[\text{CH}_2]$
Manganese (III)	1130 <i>m</i> <b>1098</b> <i>w</i> 1064 <i>m</i>	1131 <i>s</i> <b>1105</b> <i>w</i> 1062 <i>m</i>		<b>1097</b> <i>m</i> 1066 <i>m</i>	$\nu(\text{C}-\text{C})$
	935 <i>w</i>	933 <i>w</i>		943 <i>m</i>	$\rho[\text{CH}_2]$

s = strong, m = medium, w = weak,  $\nu$  = stretching,  $\delta$  = bending,  $\rho$  = rocking.

**Table 3.** the more significant Raman absorptions of synthesized palmitic and stearic acid in the region between 1200–850 cm<sup>-1</sup>.<sup>[44,92]</sup>

Palmitic Acid	Stearic Acid	Assignment
1128 s	1129 s	$\nu(\text{C}-\text{C}) + \delta(\text{C}-\text{C}-\text{C})$
1100 m	1102 m	$\nu(\text{C}-\text{C}) + \delta(\text{C}-\text{C}-\text{C})$
1062 vs	1061 s	$\nu(\text{C}-\text{C}) + \delta(\text{C}-\text{C}-\text{C})$
1052 s		$\nu(\text{C}-\text{C}) + \delta(\text{C}-\text{C}-\text{C})$
1027 w		$\nu(\text{C}-\text{C}) + \delta(\text{C}-\text{C}-\text{C})$
1008 vw	908 w	$\nu(\text{C}-\text{C})$ (carboxyl)
910 w	891 m	$\rho(\text{CH}_3) + \nu(\text{C}-\text{C})$
891 m		$\rho(\text{CH}_3) + \nu(\text{C}-\text{C})$

s = strong, m = medium, w = weak, V = stretching,  $\delta$  = bending,  $\rho$  = rocking.

Raman spectra of metal soaps show some differences with respect to pure fatty acids especially in the region between 1700 and 200 cm<sup>-1</sup>. In this range, three regions are commonly taken into consideration:

- the region between 1675 and 1640 cm<sup>-1</sup> allows the identification of unsaturated fatty acid; it was found that the C=C stretching vibration of oleic acid appears around 1656 cm<sup>-1</sup>.<sup>[92]</sup>
- the region between 1120 and 1040 cm<sup>-1</sup>, related to C–C stretching vibrations, allows the discrimination between carbon chain lengths both for fatty acids and metal carboxylates. For example, here it is possible to distinguish between palmitic and stearic acid since their bands are found at 1098 and 1104 cm<sup>-1</sup> respectively.<sup>[92]</sup>
- the region below 900 and 950 cm<sup>-1</sup>, allows the discrimination of di-acids, such as azelaic acid, with the presence at 906 cm<sup>-1</sup> of a CH<sub>2</sub> rocking vibration. It is also used to differentiate the metal cations coordinated to the same chain length and to distinguish fatty acids from metal carboxylates.<sup>[92]</sup>

As seen for FTIR, micro-Raman analysis can be successfully adopted to identify and localise metal soaps in cross-sections.

Although the use of Raman spectroscopy may yield data for the identification of metal soaps, only few studies have examined the mineralization of lead soaps in works of art.<sup>[67,70,71,107]</sup> Among them, Platania et al. revealed mineralized lead soaps in paint cross-sections: despite the complexity of the paint matrix and the low signal-to-noise ratio, their micro-Raman data suggest the conversion of lead soaps into new mineralized phases (and highlight that the transformation was still ongoing at the moment of analysis).<sup>[70]</sup> At the same time, the presence of aged compounds, which can produce fluorescence, may cause several problems in the identification of metal soaps with Raman spectroscopy. In particular, the discrimination of bands associated to metal carboxylates become difficult since the fingerprint area is characterised by peaks overlapping.<sup>[90]</sup>

Otero and co-workers used a chemometric approach to identify both the carbon chain and the metal cation involved in metal soaps formation in real case studies.<sup>[92]</sup> The models were adjusted using the IR and Raman absorptions obtained from metal soaps prepared ad hoc in the laboratory. Thus, the data

obtained in paint samples case studies can be plotted in a PCA (Principal Components Analysis) model, in order to obtain information regarding the chemical nature of metal soaps.<sup>[59,92]</sup>

### 3.7. X-Ray Diffraction Spectrometry (XRD)

XRD is an essential analytical method for the identification of crystalline metal soaps.<sup>[44]</sup> Robinet and Corbeil listed tables diffraction data from metal soaps synthesised using different fatty acids. Table 4 and 5 summarise XRD data of synthesised lead palmitate and zinc stearates.<sup>[44]</sup>

**Table 4.** X-ray powder diffraction data for lead palmitate, [C<sub>16</sub>H<sub>31</sub>O<sub>2</sub>]<sub>2</sub>Pb after Ref. [44].

d <sub>obs</sub> [nm]	I/I <sub>0</sub> [%]	d <sub>obs</sub> [nm]	I/I <sub>0</sub> [%]
4.474	100	0.3649	2.4
2.258	56.5	0.3614	0.8
15.083	52.5	0.3572	0.4
11.321	21.1	0.3541	1.1
0.9057	19.5	0.3486	2.4
0.7549	7.4	0.3424	0.5
0.6472	8.4	0.3397	1.5
0.5663	3.7	0.3327*	1.5
0.5037	5.1	0.3237	2.7
0.4535	3.3	0.3185	0.5
0.4120	2.0	0.3114	1.7
0.4069	7.1	0.3044	0.2
0.4001	1.4	0.3021	2.7
0.3963	0.6	0.2972	1.7
0.3915	2.1	0.2909	1.3
0.3862	0.7	0.2832	1.7
0.3803	1.3	0.2781	1.5
0.3778	0.9	0.2718	1.6
0.3743	0.4	0.2666	2.6
0.3677	1.7		

\*peak overlapping with peak from internal standard (mica).

**Table 5.** X-ray powder diffraction data for zinc palmitate, [C<sub>16</sub>H<sub>35</sub>O<sub>2</sub>]<sub>2</sub>Zn after.<sup>[44]</sup>

d <sub>obs</sub> [nm]	I/I <sub>0</sub> [%]	d <sub>obs</sub> [nm]	I/I <sub>0</sub> [%]
4.248	100	0.3878	5.2
21.323	29.9	0.3800	2.3
14.204	38.2	0.3736	16.8
10.649	7.9	0.3671	0.8
0.8518	12.0	0.3579	1.4
0.7095	2.3	0.3551	3.2
0.6080	3.8	0.3327*	1.1
0.5319	0.7	0.3271	0.4
0.4726	1.9	0.3193	0.7
0.4544	5.3	0.3135	1.8
0.4493	2.0	0.3026	1.1
0.4396	5.9	0.2906	0.7
0.4260	5.9	0.2868	1.5
0.4099	2.5	0.2721	0.7
0.3920	10.4	0.2700	1.2
4.248	100	0.3878	5.2
21.323	29.9	0.3800	2.3
14.204	38.2	0.3736	16.8
10.649	7.9	0.3671	0.8
0.8518	12.0	0.3579	1.4

\*peak overlapping with peak from internal standard (mica).

Both fatty acid and metal ion influence XRD spectra. The distinction between species is possible only if the metal soap analysed is present in its crystalline form.<sup>[108]</sup>

Garrappa et al. report the use of XRD and FTIR together to monitor the changes related to carboxylate formation and the passage from the amorphous to crystalline phase that depends on RH. The discrepancy between XRD transmission and reflection data is due to differences in analysed areas and in the pigment particle shape and size. It was observed that in reflection mode, the irradiated volume is very small and covers only a very thin upper layer of paint film while in transmission mode, the incident beam passes through the whole thickness of the paint film.<sup>[16]</sup> To the best of our knowledge, the number of studies regarding metal soaps analysed by XRD is limited, due to the several limitations imposed by the technique. XRD patterns must be measured with equipment able to resolve lines at low angles since the most characteristic signals of various metal soaps are present in this region, as illustrated in tables 4 e 5.<sup>[44]</sup> Moreover, XRD has a detection limit of about 1 % by volume.<sup>[109]</sup> Regarding the acquisition of diffractograms on paintings samples, some studies report the application of XRD in reflection mode: in this way, the area analysed by X-Rays at low angles is very small and it represents only the upper layer of the film.<sup>[16,34,50]</sup> On the contrary, if XRD transmission mode is employed, the incident beams pass through the entire thickness of the paint film, giving complex results from the entire multi-layered.

Garrappa et al., in a recent study, have used X-ray powder micro-diffraction ( $\mu$ -XRPD) to perform a completely non-invasive study of crystal structure of pigments and degradation products in miniature portraits.<sup>[8]</sup> The technique requires the use of a short monocapillary (135 mm).<sup>[110]</sup> For the first time, crystalline lead carboxylates were identified in miniatures, thanks to their characteristic diffraction lines in the low angle region. The very sharp appearance of peaks suggests that lead soaps are probably organised in a highly crystalline structure. Among the advantages, the authors clearly underline as it is essential to correct the sample displacement and maintain its orientation. Even a small change during the ongoing measurement, can have a significant impact on the line position.<sup>[8]</sup>

To overcome the many limitations of the technique, new strategies have been developed in the use XRD analysis. As for FTIR,  $\mu$ SR-XRD has been employed to obtain high-quality data.<sup>[105]</sup> Often XRD and FTIR are used together in the study of metal soaps<sup>[16,39,58,105]</sup> but several studies show how the incomplete crystallisation of these compounds may produce ambiguous results. XRD may suggest aggregates with crystalline features while FTIR spectra of the same samples exhibit broad band associated with amorphous phase<sup>[39,58]</sup> which underlines a disordered system.

### 3.8. Nuclear Magnetic Resonance (NMR)

NMR based techniques have been successfully employed in several ways to investigate the chemical and physical nature of compounds present in paint films, among them metal soaps.

A detailed and precise review on the use of NMR to study structure, reactivity and dynamics of lead soaps has been recently written by Catalano et al.<sup>[111]</sup> Their review deals with many applications of solution-state NMR spectroscopy, high-resolution NMR (HR NMR), and solid-state NMR (ssNMR).<sup>[111]</sup>

ssNMR may provide crucial crystallographic and structural information on samples affected by saponification and was employed to explain structural features of lead soaps. In particular, <sup>207</sup>Pb ssNMR was useful to determine the coordination environment of the lead centre in lead soaps<sup>[111]</sup> and to distinguish between hexadecanoate and octadecanoate anions.<sup>[35]</sup> It has been demonstrated that these mixed lead soaps, in a model experiment simulating a historic paint layer, are formed and both lead carboxylates are present in one crystalline phase.<sup>[112,113]</sup> Figure 4 reports <sup>207</sup>Pb WURST-CPMG spectra of three different lead soaps, lead, octanoate, lead palmitate and lead azelate, obtained with proper arrangements in order to overcome the problems of sensitivity (i.e. uniform-rate and smooth-truncation (WURST) and WURST-based Carr-Purcell-Meiboom-Gill (CPMG)).<sup>[114]</sup>

The formation of the ionic network seems to take place in early stages after paint application: research by Verhoeven et al. showed that lead pigments and carboxylates could be detected within 5 years of synthesis.<sup>[115]</sup> Keune and Boon underlined that early lead soap formation may be considered as vital for the stability of oil paintings.<sup>[84]</sup>

Unilateral NMR may be helpful in determining the open porosity (i.e. void fraction or 'empty' spaces that may be filled by water or organic solvents in contact with the paint film) of different materials.<sup>[116,117]</sup> Since open porosity may favour the diffusion of water and solvents in multi-layered paint films, it is crucial in metal soaps formation.

Liu et al. employed unilateral NMR (with a proton Larmor frequency of 18 MHz at 0.36 T) to evaluate how the water absorption and the open porosity of oil paints can be affected by zinc and lead whites in different concentrations, and by the

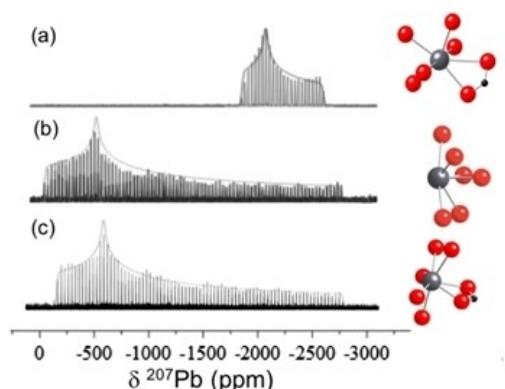


**Figure 4.** The local lead coordination environment and the <sup>207</sup>Pb WURST-CPMG spectra for (a) a long-chain carboxylate, lead octanoate, (b) lead azelate and (c) a long-chain lead carboxylate, lead palmitate. Reproduced. This Agreement between Dr. Francesca Caterina Izzo ("You") and John Wiley and Sons ("John Wiley and Sons") consists of your license details and the terms and conditions provided by John Wiley and Sons and Copyright Clearance Center. Copyright holders: J. Catalano, V. Di Tullio, M. Wagner, N. Zumbulyadis, S. A. Centeno, C. Dybowski.

**Table 6.** characteristic positive secondary fragment ions of lead soaps based on Ref. [125, 126].

[m/z]	Fragment ion	Assignment
393–395	[Pb + CHOOCR(COO)] <sup>+</sup>	Lead soaps of azelaic acid
461–463	[Pb + R(COO)] <sup>+</sup>	Lead soaps of palmitic acid
489–491	[Pb + R(COO)] <sup>+</sup>	Lead soaps of stearic acid

presence of the aluminium stearate as an additive, by measuring the transverse relaxation times in the cured paint samples before and after water absorption were measured.<sup>[65]</sup> In addition, single-sided NMR can be used to perform in situ and non-invasive analysis to monitor the penetration depth, the chemical and physical effects of solvents, solutions, and suspensions, when various surface-cleaning techniques are applied.<sup>[111]</sup>

Despite the several specific advantages related to the unique ability to probe metal coordination, each NMR technique has disadvantages which cannot be underestimated due to sampling. Its sensitivity is considered quite low in comparison to other spectroscopic techniques, and current instrumentation requires relatively large samples which are not always available in heritage applications.<sup>[111]</sup>

### 3.9. Gas Chromatography Coupled with Mass Spectrometry (GC-MS)

GC-MS is widely used in Heritage and Conservation Science for the characterisation of organic compounds present in paintings and archaeological findings.<sup>[118]</sup> GC-MS can successfully detect fatty acids in paint micro-samples, according to different derivatisation procedures, which enable the transformation of each fatty acid from the lipidic matrix in volatile compounds (such as methyl ester or tri-methyl-silyl derivatives).<sup>[52,53]</sup> For this reason, GC-MS is, in theory, an ideal method for the identification of the organic fraction of metal soaps. Nevertheless, it is not easy to elucidate if these fatty acids were originally present as metal soaps, free fatty acids or glycerides.<sup>[44]</sup> Despite numerous studies on the identification of lipid binders and their oxidation, hydrolysis and degradation products by GC-MS, not many papers have been published on the identification of metal soaps.

In 2002, a study by van den Berg suggested that, during drying and curing of an oil painting, two different “GC-MS phases” can be formed: the “mobile phase”, made up of oxidised and de-esterified fatty acids, glycerol, mono-, di- and triacylglycerols, and the “stationary phase”, characterized by a cross-linked polymeric system.<sup>[52]</sup>

Generally, GC-MS methodologies involve the use of derivatisation agents which transform the fatty acids from both phases. Thus, it is not easy to correlate the presence of fatty acids if complex mixtures of carboxylates, acylglycerols and free fatty acids are present.<sup>[119]</sup> La Nasa and co-workers developed a GC-MS approach to identify and quantify metal soaps formed in oil samples present in the mobile phase. The analytical

procedure proposed can be performed on a single sample aliquot following two steps consecutively: two derivatisation agents were employed in order to identify free (di)fatty acids and metal carboxylates (using N,O-bis(trimethylsilyl) trifluoroacetamide containing 1% of trimethylchlorosilane, commercially known as BSTFA + TMCS) and only free (di)carboxylic acids (using 1,1,1,3,3,3-hexamethyldisilazane, HMDS).<sup>[119]</sup> This procedure was adopted by Platania and co-workers to analyse sample containing lead soaps and GC-MS analyses allowed the identification of lipid materials and provide a support to the previous spectroscopic study.<sup>[90]</sup>

The results obtained from GC-MS give information only regarding the organic fraction.

### 3.10. Secondary Ion Mass Spectrometry (SIMS)

SIMS applications on metal soaps, as static and time-of-flight SIMS (TOF-SIMS), were largely adopted by Keune and co-workers who reported the potential of this technique to study cross-sections from 15<sup>th</sup>–20<sup>th</sup> century paintings.<sup>[120]</sup> Thanks to its versatility, SIMS is able to identify, localise and map both organic and inorganic components (such as fatty acids and metal cations from metal soaps) in complex, heterogenous and multi-layered paint systems.<sup>[4,6,22,34,84,120–124]</sup> Moreover, it can be used both in the imaging mode and as an analytical MS tool. In the first case, images of cross-sections, characterized by the distribution of selected mass of interest (m/z) in painted layers, are produced,<sup>[120]</sup> while in the second case, it identifies organic and inorganic components through their mass spectra.<sup>[10,34,66,84,101]</sup> Positive and negative ion modes can provide different information coming from inorganic and organic materials, respectively.<sup>[125]</sup>

As for the other techniques reviewed in this paper, the attention was focused on lead and zinc soaps. Figure 5 illustrates an example of analytical study of a cross-section from *The Anatomy Lesson of Dr. Nicolas Tulp* by Rembrandt: the presence of lead soaps was elucidated by complementary analysis of microscopy, SEM-BSE, FTIR and SIMS images combined with the positive SIMS spectrum of lead palmitate.<sup>[6]</sup>

The characteristic positive secondary fragment ions from lead palmitates, azelates and stearates can be discriminated by SIMS analysis as reported in Table 6.<sup>[125,126]</sup>

Zinc soaps are unstable under SIMS ionization according to Keune. It is possible to avoid this by applying an ultra-thin gold coating on samples: the coating enhances positive and negative secondary ion yields of lipids. In this way, a spatial correlation of fatty acids and zinc inside the studied aggregates was observed.<sup>[120]</sup>

Applications of TOF-SIMS on real paint samples took into consideration *Portrait of Nicolaes van Bambeeck* by Rembrandt (1641) and *Saint Wilgefortis Triptych* by Hieronymus Bosh (~1497): both the paintings were affected by lead soap formation. In the first case, the interaction between oil medium and lead white was suggested by the overlap of images provide by cluster-TOF-SIMS.<sup>[105]</sup> In the second case study, the saponification process was confirmed taking into consideration the

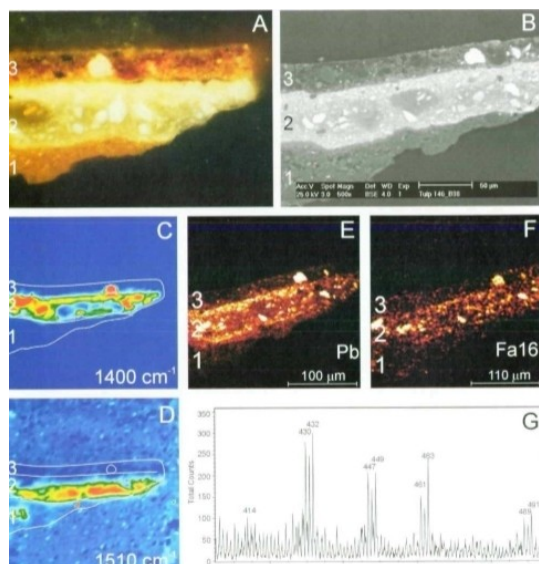


**Figure 5.** Analytical imaging studies of paint cross-section MII146 B38 taken from The Anatomy Lesson of Dr. Nicolaes Tulp by Rembrandt van Rijn (1632). White light microscopic image (A) and back scattered electron image (BSE-image) (B) reveal the layer buildup and granulometry: FTIR images represent carbonate carbonyl groups at  $1400\text{ cm}^{-1}$  (C) and lead carboxylates at  $1510\text{ cm}^{-1}$  (D) (red represents high and blue low intensity). An outline illustrates the three layers and the circle in layer 3 is indicative for the large lead white particle in this layer. SIMS-images represent lead (+:  $m/z$  206–208) (E) and deprotonated palmitic acid (–:  $m/z$  253) (F). A part of the positive SIMS spectrum presents  $\text{Pb}_3\text{O}$  at  $m/z$  426–432.  $\text{Pb}_3\text{O}_2\text{H}$  at  $m/z$  443–449.  $\text{PhOOC}(\text{CH}_2)_{14}\text{CH}_3$  at  $m/z$  461–463 and  $\text{PbOOC}(\text{CH}_2)_{10}\text{CH}_3$  at  $m/z$  489–491 (G). Reproduced from the PhD thesis “Binding Medium, Pigments and Metal Soaps Characterised and Localised in Paint Cross-Sections, University of Amsterdam 2005, with the permission from Katrien Keune (copyright holder).

specific fatty acid spectral fingerprint region (from 200 to  $300\text{ m/z}$ , both positive and negative mode).<sup>[125]</sup>

SIMS is considered as superficial and non-destructive technique, since only the upper atomic layer of samples is probed and no structural damage is visible in the cross-sections.<sup>[6,120]</sup> When using a liquid metal ion gun, the lateral image resolution is about  $1\text{ }\mu\text{m}$ . SIMS can detect elements in traces and the detection limit (around  $0.001\text{ wt}\%$ ) is strictly depending on the ionisation potential and matrix effects. Therefore, the technique is very sensitive to the irregularity of the surface and an accurate preparation of sample is required.<sup>[6]</sup> In addition, SIMS has some limitations in the detection of oxidation and degradation products in an oil matrix, probably because their low relative abundance.

#### 4. Conclusions and Outlook

In this work, the major analytical techniques used to study metal soap formation in paintings have been reported, together with a description of the advantages and limitations associated with each. In the text, guides useful for the interpretation of data have been provided in an attempt to aim future applications of analytical techniques to investigations. No single technique can provide a complete chemical description of the

structure and complex mechanisms of soap formation. Instead, we believe that it is through a complementary and multi-analytical approach that insights regarding metal soaps will be gained in the future. The microscopic stratigraphic analysis of paint samples will continue to help in unravelling the processes that occur in paint films – and instrumental advances regarding micro spectroscopic analysis are likely to play an important role in identifying early stages of soap formation and in the mapping of crystalline soaps within paint samples. Furthermore, mechanistic studies and information from model samples and the evolution of degradation products in the inorganic-organic systems which are found in paint will continue to be important in assessing the kinetics of soap formation and stability of metal soaps in works of art. While non-invasive in situ methods continue to be popular for investigations of paintings, they are inherently limited in identifying complex systems where stratigraphic and specific information related to organic and inorganic salts are required. Nonetheless sampling of any painting and specifically of metal soaps also comes with limitations in that samples may not be representative of the multiple layers in a painting. The implications of analytical results also require careful evaluation which implies balanced assessment of condition, preventive and remedial treatments, and suitable methods for evaluation of cleaning.

#### Acknowledgements

The authors acknowledge PhD. Dr. J. J. Hermans, PhD. Dr. K. Keune, PhD. Dr. P. Noble and the Canadian Conservation Institute for providing us the permission to reproduce their images.

#### Conflict of Interest

The authors declare no conflict of interest.

**Keywords:** conservation science · FT-IR · ion migration · metal soaps · paint degradation · Raman spectroscopy

- [1] P. Noble, in: *Met. Soaps Art Conserv. Res.* (Eds.: F. Casadio, K. Keune, P. Noble, A. Van Loon, E. Hendriks, S. A. Centeno, G. Osmond), Springer International Publishing, Cham, **2019**, pp. 1–22.
- [2] M. Clarke, J. J. Boon, Eds., *A Multidisciplinary NWO PRIORITEIT Project on Molecular Aspects of Ageing in Painted Works of Art: Final Report and Highlights 1995–2002*, FOM Institute AMOLF, Amsterdam, **2003**.
- [3] P. Noble, J. Wadum, J. J. Boon, *Art Matters* **2001**, 1.
- [4] J. J. Boon, J. van der Weerd, K. Keune, P. Noble, J. Wadum: *Mechanical and chemical changes in Old Master paintings: dissolution, metal soap formation and remineralization processes in lead pigmented ground/intermediate paint layers of 17th century paintings*. In: 13th triennial meeting Rio de Janeiro 22–27 September 2002: icom committee for conservation/ed. R. Vontobel, James & James, **2002**, pp. 401–406.
- [5] P. Noble, A. van Loon, J. J. Boon, **2005**, p. 9.
- [6] K. Keune, *Binding Medium, Pigments and Metal Soaps Characterised and Localised in Paint Cross-Sections*, PhD thesis – Universiteit van Amsterdam, Amsterdam, **2005**.
- [7] J. J. Boon, F. Hoogland, K. Keune, H. M. Parkin, H. Mar Parkin, AIC, **2007**, pp. 16–23.



- [8] S. Garrappa, D. Hradil, J. Hradilová, E. Kočí, M. Pech, P. Bezdička, S. Švarcová, *Anal. Bioanal. Chem.* **2021**, *413*, 263–278.
- [9] K. Muir, A. Langley, A. Bezur, F. Casadio, J. Delaney, G. Gautier, *J. Am. Inst. Conserv.* **2013**, *52*, 156–172.
- [10] J. Van Der Weerd, M. Geldof, L. Struik van der Loeff, R. M. A. Heeren, J. J. Boon, *Z Für Kunsttechnol. Konserv. ZKK* **2002**, *17*, 407–416.
- [11] F. C. Izzo, B. Ferriani, K. J. V. den Berg, H. Van Keulen, E. Zendri, *J. Cult. Herit.* **2014**, *15*, 557–563.
- [12] F. C. Izzo, K. J. van den Berg, H. van Keulen, B. Ferriani, E. Zendri, in: *Issues Contemp. Oil Paint* (Eds.: K. J. van den Berg, A. Burnstock, M. de Keijzer, J. Krueger, T. Learner, A. de Tagle, G. Heydenreich), Springer International Publishing, Cham, **2014**, pp. 75–104.
- [13] F. Gabrieli, F. Rosi, A. Vichi, L. Cartechini, L. Pensabene Buemi, S. G. Kazarian, C. Miliani, *Anal. Chem.* **2017**, *89*, 1283–1289.
- [14] J. Salvant, M. Walton, D. Kronkright, C.-K. Yeh, F. Li, O. Cossairt, A. K. Katsaggelos, in: *Met. Soaps Art Conserv. Res.* (Eds.: F. Casadio, K. Keune, P. Noble, A. Van Loon, E. Hendriks, S. A. Centeno, G. Osmond), Springer International Publishing, Cham, **2019**, pp. 375–391.
- [15] W. Faubel, R. Simon, S. Heissler, F. Friedrich, P. G. Weidler, H. Becker, W. Schmidt, *J. Anal. At. Spectrom.* **2011**, *26*, 942.
- [16] S. Garrappa, E. Kočí, S. Švarcová, P. Bezdička, D. Hradil, *Microchem. J.* **2020**, *156*, 104842.
- [17] A. Artesani, *Mater. Chem. Phys.* **2020**, *255*, 123640.
- [18] M. Thoury, A. Van Loon, K. Keune, J. J. Hermans, M. Réfrégiers, B. H. Berrie, in: *Met. Soaps Art Conserv. Res.* (Eds.: F. Casadio, K. Keune, P. Noble, A. Van Loon, E. Hendriks, S. A. Centeno, G. Osmond), Springer International Publishing, Cham, **2019**, pp. 211–225.
- [19] A. Van Loon, R. Hoppe, K. Keune, J. J. Hermans, H. Diependaal, M. Bisschoff, M. Thoury, G. van der Snickt, in: *Met. Soaps Art Conserv. Res.* (Eds.: F. Casadio, K. Keune, P. Noble, A. Van Loon, E. Hendriks, S. A. Centeno, G. Osmond), Springer International Publishing, Cham, **2019**, pp. 359–373.
- [20] L. E. Raven, M. Bisschoff, M. Leeuwestein, M. Geldof, J. J. Hermans, M. Stols-Witlox, K. Keune, in: *Met. Soaps Art Conserv. Res.* (Eds.: F. Casadio, K. Keune, P. Noble, A. Van Loon, E. Hendriks, S. A. Centeno, G. Osmond), Springer International Publishing, Cham, **2019**, pp. 343–358.
- [21] K. Keune, R. P. Kramer, S. Stangier, M. H. van Eikema Hommes, in: *Met. Soaps Art Conserv. Res.* (Eds.: F. Casadio, K. Keune, P. Noble, A. Van Loon, E. Hendriks, S. A. Centeno, G. Osmond), Springer International Publishing, Cham, **2019**, pp. 107–121.
- [22] M. Cotte, E. Checroun, W. De Nolf, Y. Taniguchi, L. De Viguerie, M. Burghammer, P. Walter, C. Rivard, M. Salomé, K. Janssens, J. Susini, *Stud. Conserv.* **2017**, *62*, 2–23.
- [23] F. Casadio, K. Keune, P. Noble, A. van Loon, E. Hendriks, S. A. Centeno, G. Osmond, *Metal Soaps in Art: Conservation and Research*, Springer International Publishing, **2019**.
- [24] J. Liang, D. A. Scott, *Stud. Conserv.* **2014**, *59*, 391–403.
- [25] N. Salvadó, S. Butí, J. Nicholson, H. Emerich, A. Labrador, T. Pradell, *Talanta* **2009**, *79*, 419–428.
- [26] R. Mazzeo, S. Prati, M. Quaranta, E. Joseph, E. Kendix, M. Galeotti, *Anal. Bioanal. Chem.* **2008**, *392*, 65–76.
- [27] S. Švarcová, E. Kočí, J. Plocek, A. Zhankina, J. Hradilová, P. Bezdička, *J. Cult. Herit.* **2019**, *38*, 8–19.
- [28] M. J. Plater, B. De Silva, T. Gelbrich, M. B. Hursthouse, C. L. Higgitt, D. R. Saunders, *Polyhedron* **2003**, *22*, 3171–3179.
- [29] K. Helwig, J. Poulin, M.-C. Corbeil, E. Moffatt, D. Duguay, in: *Issues Contemp. Oil Paint* (Eds.: K. J. van den Berg, A. Burnstock, M. de Keijzer, J. Krueger, T. Learner, A. de Tagle, G. Heydenreich), Springer International Publishing, Cham, **2014**, pp. 167–184.
- [30] L. Fuster-López, F. C. Izzo, M. Piovesan, D. J. Yusá-Marco, L. Sporni, E. Zendri, *Microchem. J.* **2016**, *124*, 962–973.
- [31] L. Fuster-López, F. C. Izzo, V. Damato, D. J. Yusá-Marco, E. Zendri, *J. Cult. Herit.* **2019**, *35*, 225–234.
- [32] L. Carlyle, *The Artist's Assistant: Oil Painting Instruction Manuals and Handbooks in Britain, 1800–1900*, Archetype Publications, **2001**.
- [33] M. Cotte, E. Checroun, J. Susini, P. Walter, *Appl. Phys. A* **2007**, *89*, 841–848.
- [34] K. Keune, J. J. Boon, *Stud. Conserv.* **2007**, *52*, 161–176.
- [35] J. Catalano, A. Murphy, Y. Yao, G. P. A. Yap, N. Zumbulyadis, S. A. Centeno, C. Dybowski, *Dalton Trans.* **2015**, *44*, 2340–2347.
- [36] G. Osmond, in: *Met. Soaps Art Conserv. Res.* (Eds.: F. Casadio, K. Keune, P. Noble, A. Van Loon, E. Hendriks, S. A. Centeno, G. Osmond), Springer International Publishing, Cham, **2019**, pp. 25–46.
- [37] G. Osmond, in: *Issues Contemp. Oil Paint* (Eds.: K. J. van den Berg, A. Burnstock, M. de Keijzer, J. Krueger, T. Learner, A. de Tagle, G. Heydenreich), Springer International Publishing, Cham, **2014**, pp. 263–281.
- [38] D. Rogala, S. Lake, C. Maines, M. Mecklenburg, *J. Am. Inst. Conserv.* **2010**, *49*, 96–113.
- [39] J. J. Hermans, K. Keune, A. Van Loon, P. D. Iedema, in: *Met. Soaps Art Conserv. Res.* (Eds.: F. Casadio, K. Keune, P. Noble, A. Van Loon, E. Hendriks, S. A. Centeno, G. Osmond), Springer International Publishing, Cham, **2019**, pp. 47–67.
- [40] E. Pratali, “Zinc oxide grounds in 19th and 20th century oil paintings and their role in picture degradation processes”, *CeROArt* [Online], EGG 3 | 2013, Online since 10 May 2013, connection on 06 September 2021. URL: <http://journals.openedition.org/ceroart/3207>; DOI: <https://doi.org/10.4000/ceroart.3207>.
- [41] G. Osmond, B. Ebert, J. Drennan, *AICCM Bull.* **2013**, *34*, 4–14.
- [42] C. A. Maines, D. V. Rogala, S. Lake, M. F. Mecklenburg, **2011**, DOI 10.1557/opl.2011.733.
- [43] G. Osmond, *AICCM Bull.* **2012**, *33*, 20–29.
- [44] L. Robinet, M.-C. Corbeil, *Stud. Conserv.* **2003**, *48*, 23–40.
- [45] C. S. Tumosa, “A Brief History of Aluminum Stearate as a Component of Paint,” can be found under <https://cool.culturalheritage.org/waac/wn/wn23/wn23-3/wn23-304.html>, **2001**.
- [46] A. Burnstock, K. J. van den Berg, S. de Groot, L. Wijnberg, In *Reprints of the Modern Paints Uncovered conference*, London **2006**, 177–188.
- [47] J. J. Hermans, Metal Soaps in Oil Paint. Structure, Mechanisms and Dynamics, University of Amsterdam, Faculty of Science (FNWI), Van't Hoff Institute for Molecular Sciences (HIMS), **n.d.**
- [48] J. J. Hermans, K. Keune, A. van Loon, R. W. Corkery, P. D. Iedema, *RSC Adv.* **2016**, *6*, 93363–93369.
- [49] J. J. Hermans, K. Keune, A. van Loon, P. D. Iedema, *Phys. Chem. Chem. Phys.* **2016**, *18*, 10896–10905.
- [50] J. J. Hermans, K. Keune, A. van Loon, P. D. Iedema, *J. Anal. At. Spectrom.* **2015**, *30*, 1600–1608.
- [51] J. J. Hermans, K. Keune, A. van Loon, R. W. Corkery, P. D. Iedema, *Polyhedron* **2014**, *81*, 335–340.
- [52] J. D. J. van den Berg, *Analytical Chemical Studies on Traditional Linseed Oil Paints*, FOM-Institute AMOLF, **2002**.
- [53] F. C. Izzo, 20th Century Artists' Oil Paints: A Chemical-Physical Survey, Ca' Foscari, Venezia, **2011**.
- [54] D. Erhardt, C. S. Tumosa, M. F. Mecklenburg, *Stud. Conserv.* **2005**, *50*, 143–150.
- [55] J. J. Hermans, L. Baij, M. Koenis, K. Keune, P. D. Iedema, S. Woutersen, *Sci. Adv.* **2019**, *5*, eaaw3592.
- [56] L. Baij, J. Hermans, B. Ormsby, P. Noble, P. Iedema, K. Keune, *Herit. Sci.* **2020**, *8*, 43.
- [57] A. Van Loon, Color Changes and Chemical Reactivity in Seventeenth-Century Oil Paintings, University of Amsterdam, **2008**.
- [58] M. G. MacDonald, M. R. Palmer, M. R. Suchomel, B. H. Berrie, *ACS Omega* **2016**, *1*, 344–350.
- [59] J. Lee, I. Bonaduce, F. Modugno, J. La Nasa, B. Ormsby, K. J. van den Berg, *Microchem. J.* **2018**, *138*, 282–295.
- [60] F. Modugno, F. Di Gianvincenzo, I. Degano, I. D. van der Werf, I. Bonaduce, K. J. van den Berg, *Sci. Rep.* **2019**, *9*, 5533.
- [61] J. J. Hermans, Metal Soaps in Oil Paint. Structure, Mechanisms and Dynamics, University of Amsterdam, Faculty of Science (FNWI), Van't Hoff Institute for Molecular Sciences (HIMS), **2017**.
- [62] A. Burnstock, in: *Met. Soaps Art Conserv. Res.* (Eds.: F. Casadio, K. Keune, P. Noble, A. Van Loon, E. Hendriks, S. A. Centeno, G. Osmond), Springer International Publishing, Cham, **2019**, pp. 243–262.
- [63] G. Eumelen, E. Bosco, A. S. J. Suiker, A. van Loon, P. Iedema, *J. Mech. Phys. Solids* **2019**, *132*, 103683.
- [64] J. Hermans, G. Osmond, A. van Loon, P. Iedema, R. Chapman, J. Drennan, K. Jack, R. Rasch, G. Morgan, Z. Zhang, M. Monteiro, K. Keune, *Microsc. Microanal.* **2018**, *24*, 318–322.
- [65] X. Liu, V. Di Tullio, Y.-C. Lin, V. De Andrade, C. Zhao, C.-H. Lin, M. Wagner, N. Zumbulyadis, C. Dybowski, S. A. Centeno, Y. K. Chen-Wiegart, *Sci. Rep.* **2020**, *10*, 18320.
- [66] P. Noble, J. J. Boon, in *Paint. Spec. Group*, Richmond, VA, USA, **2007**.
- [67] C. Higgitt, M. Spring, D. Saunders, *Natl. Gallery Tech. Bull.* **2003**, *24*, 75–95.
- [68] G. Osmond, K. Keune, J. J. Boon, *AICCM Bull.* **2005**, *29*, 37–46.
- [69] E. J. Henderson, K. Helwig, S. Read, S. M. Rosendahl, *Herit. Sci.* **2019**, *7*, 71.
- [70] E. Platania, N. L. W. Streeton, A. Vila, D. Buti, F. Caruso, E. Uggerud, *Spectrochim. Acta* **2020**, *228*, 117844.

- [71] J. Van Der Weerd, J. J. Boon, M. Geldof, R. M. A. Heeren, P. Noble, Z. *Fiir Kunsttechnol. Konserv. ZKK* **2002**, *16*, 36–51. >
- [72] S. Hageraats, K. Keune, M. Réfrégiers, A. van Loon, B. Berrie, M. Thoury, *Anal. Chem.* **2019**, *91*, 14887–14895.
- [73] A. Nevin, A. Cesaratto, S. Bellei, C. D'Andrea, L. Toniolo, G. Valentini, D. Comelli, *Sensors* **2014**, *14*, 6338–6355.
- [74] L. Giorgi, A. Nevin, L. Nodari, D. Comelli, R. Alberti, M. Gironda, S. Mosca, E. Zendri, M. Piccolo, F. C. Izzo, *Spectrochim. Acta* **2019**, *219*, 530–538.
- [75] V. Gonzalez, D. Gourier, T. Calligaro, K. Toussaint, G. Wallez, M. Menu, *Anal. Chem.* **2017**, *89*, 2909–2918.
- [76] A. Artesani, S. Bellei, V. Capogrosso, A. Cesaratto, S. Mosca, A. Nevin, G. Valentini, D. Comelli, *Appl. Phys. A* **2016**, *122*, 1053.
- [77] A. Artesani, F. Gherardi, A. Nevin, G. Valentini, D. Comelli, *Materials* **2017**, *10*, 340.
- [78] L. Bertrand, M. Réfrégiers, B. Berrie, J.-P. Échard, M. Thoury, *Analyst* **2013**, *138*, 4463–4469.
- [79] D. Comelli, A. Artesani, A. Nevin, S. Mosca, V. Gonzalez, M. Eveno, G. Valentini, *Materials* **2017**, *10*, 1335.
- [80] P. A. Rodnyi, I. V. Khodyuk, *Opt. Spectrosc. n.d.*, *111*, 776–785.
- [81] *Spectrochim. Acta* **2019**, *219*, 504–508.
- [82] D. V. Rogala, in: *Met. Soaps Art Conserv. Res.* (Eds.: F. Casadio, K. Keune, P. Noble, A. Van Loon, E. Hendriks, S. A. Centeno, G. Osmond), Springer International Publishing, Cham, **2019**, pp. 315–328.
- [83] *Microchem. J.* **2018**, *139*, 467–474.
- [84] K. Keune, J. J. Boon, *Anal. Chem.* **2004**, *76*, 1374–1385.
- [85] K. Keune, A. van Loon, J. Boon, *Microsc. Microanal. Off.* **2011**, *17*, 696–701.
- [86] G. Osmond, Zinc Oxide-Centred Deterioration of Modern Artists' Oil Paint and Implications for the Conservation of Twentieth Century Paintings, PhD Thesis, The University of Queensland, Australian Institute for Bioengineering and Nanotechnology, **2014**.
- [87] C. Romano, T. Lam, G. A. Newsome, J. A. Taillon, N. Little, J. Tsang, *Stud. Conserv.* **2020**, *65*, 14–27.
- [88] J. van der Weerd, R. M. A. Heeren, J. J. Boon, *Stud. Conserv.* **2004**, *49*, 193–210.
- [89] F. Rosi, A. Federici, B. G. Brunetti, A. Sgamellotti, S. Clementi, C. Miliani, *Anal. Bioanal. Chem.* **2011**, *399*, 3133–3145.
- [90] E. Platania, N. L. W. Streeton, A. Lluveras-Tenorio, A. Vila, D. Buti, F. Caruso, H. Kutzke, A. Karlsson, M. P. Colombini, E. Uggerud, *Microchem. J.* **2020**, *156*, 104811.
- [91] M. Beerse, K. Keune, P. Iedema, S. Woutersen, J. Hermans, *ACS Appl. Polym. Mater.* **2020**, *2*, 5674–5685.
- [92] V. Otero, D. Sanches, C. Montagner, M. Vilarigues, L. Carlyle, J. A. Lopes, M. J. Melo, *J. Raman Spectrosc.* **2014**, *45*, 1197–1206.
- [93] Q. Dou, K. M. Ng, *Powder Technol.* **2016**, *301*, 949–958.
- [94] C. Miliani, F. Rosi, A. Daveri, B. G. Brunetti, *Appl. Phys. A* **2012**, *106*, 295–307.
- [95] L. Nodari, P. Ricciardi, *Herit. Sci.* **2019**, *7*, 7.
- [96] F. Casadio, L. Toniolo, *J. Cult. Herit.* **2001**, *2*, 71–78.
- [97] M. R. Derrick, D. Stulik, J. M. Landry, *Infrared Spectroscopy in Conservation Science*, Getty Publications, **2000**.
- [98] L. Baij, J. J. Hermans, K. Keune, P. Iedema, *Angew. Chem. Int. Ed. Engl.* **2018**, *57*, 7351–7354.
- [99] G. Gautier, A. Bezur, K. Muir, F. Casadio, I. Fiedler, *Appl. Spectrosc.* **2009**, *63*, 597–603.
- [100] J. Hermans, K. Helwig, *Appl. Spectrosc.* **2020**, *74*, 1505–1514.
- [101] R. M. A. Heeren, J. J. Boon, P. Noble, J. Wadum, J. Bridgland, J. Brown, London, **1999**, pp. 228–233.
- [102] E. Possenti, C. Colombo, M. Realini, C. L. Song, S. G. Kazarian, *Anal. Bioanal. Chem.* **2020**, DOI 10.1007/s00216-020-03016-6.
- [103] M. Spring, C. Ricci, D. A. Peggie, S. G. Kazarian, *Anal. Bioanal. Chem.* **2008**, *392*, 37–45.
- [104] Z. E. Papiak, L. Vaccari, F. Zanini, S. Sotiropoulou, *Anal. Bioanal. Chem.* **2015**, *407*, 5393–5403.
- [105] N. Salvadó, S. Buti, T. Pradell, V. Beltran, G. Cinque, J. Juanhuix, in: *Met. Soaps Art Conserv. Res.* (Eds.: F. Casadio, K. Keune, P. Noble, A. Van Loon, E. Hendriks, S. A. Centeno, G. Osmond), Springer International Publishing, Cham, **2019**, pp. 195–210.
- [106] X. Ma, V. Beltran, G. Ramer, G. Pavlidis, D. Y. Parkinson, M. Thoury, T. Meldrum, A. Centrone, B. H. Berrie, *Angew. Chem. Int. Ed.* **2019**, *58*, 11652–11656; *Angew. Chem.* **2019**, *131*, 11778–11782.
- [107] J. J. Boon, *Report. Highlights Mayerne Programme* **2006**, 21–32.
- [108] M.-C. Corbeil, L. Robinet, *Powder Diffr.* **2002**, *17*, 52–60.
- [109] B. D. Cullity, S. R. Stock, *Elements of X-Ray Diffraction*, Third Edition, New York: Prentice-Hall, **2001**.
- [110] J. Hradilová, D. Hradil, M. Pech, P. Bezdička, V. Neděla, E. Tihlaříková, P. Targowski, *Microchem. J.* **2020**, *153*, 104371.
- [111] J. Catalano, V. Di Tullio, M. Wagner, N. Zumbulyadis, S. A. Centeno, C. Dybowski, *Magn. Reson. Chem.* **2020**, DOI 10.1002/mrc.5025.
- [112] E. Kočí, J. Rohlíček, L. Kobera, J. Plocek, S. Švarcová, P. Bezdička, *Dalton Trans.* **2019**, *48*, 12531–12540.
- [113] S. Švarcová, E. Kočí, P. Bezdička, S. Garrappa, L. Kobera, J. Plocek, J. Brus, M. Štašný, D. Hradil, *Dalton Trans.* **2020**, *49*, 5044–5054.
- [114] S. T. Holmes, W. D. Wang, G. Hou, C. Dybowski, W. Wang, S. Bai, *Phys. Chem. Chem. Phys.* **2019**, *21*, 6319–6326.
- [115] M. A. Verhoeven, L. Carlyle, J. Reedijk, J. G. Haasnoot, NWO, The Hague, **2006**.
- [116] C. Rehorn, B. Blümich, *Angew. Chem. Int. Ed.* **2018**, *57*, 7304–7312; *Angew. Chem.* **2018**, *130*, 7426–7434.
- [117] V. D. Tullio, N. Zumbulyadis, S. A. Centeno, J. Catalano, M. Wagner, C. Dybowski, *ChemPhysChem* **2020**, *21*, 113–119.
- [118] M. P. Colombini, F. Modugno, *Organic Mass Spectrometry in Art and Archaeology*, John Wiley & Sons, **2009**.
- [119] J. La Nasa, F. Modugno, M. Aloisi, A. Lluveras-Tenorio, I. Bonaduce, *Anal. Chim. Acta* **2018**, *1001*, 51–58.
- [120] K. Keune, F. Hoogland, J. J. Boon, D. Peggie, C. Higgitt, *Int. J. Mass Spectrom.* **2009**, *284*, 22–34.
- [121] J. J. Boon, K. Keune, T. Learner: *Identification of pigments and media from a paint cross-section by direct mass spectrometry and high-resolution imaging mass spectrometric and microspectroscopic techniques*. In: 13th triennial meeting Rio de Janeiro 22–27 September 2002: icom committee for conservation/ed. R. Vontobel, James & James, **2002**, pp. 223–230.
- [122] K. Keune, E. Ferreira, J. Boon, in *14th Trienn. Meet. Hague Prepr.*, James and James, **2005**, p. 796.
- [123] E. S. B. Ferreira, R. Morrisson, K. Keune, J. J. Boon, in *Report. Highlights Mayerne Programme Res. Programme Mol. Stud. Conserv. Tech. Stud. Art Hist.*, The Hague:NWO, **2006**, p. 53.
- [124] J. Sanyova, S. Cersoy, P. Richardin, O. Laprévotte, P. Walter, A. Brunelle, *Anal. Chem.* **2011**, *83*, 753–760.
- [125] A. Sodo, L. Tortora, P. Biocca, A. C. Municchia, E. Fiorin, M. A. Ricci, *J. Raman Spectrosc.* **2019**, *50*, 150–160.
- [126] K. Keune, J. J. Boon, *Surf. Interface Anal.* **2004**, *36*, 1620–1628.

Manuscript received: July 10, 2021  
Revised manuscript received: July 20, 2021